Surfaces and Interfaces 42 (2023) 103502

Contents lists available at ScienceDirect

Surfaces and Interfaces

journal homepage: www.sciencedirect.com/journal/surfaces-and-interfaces

Combined use of *in situ* and *operando*-FTIR, TPR and FESEM techniques to investigate the surface species along the simultaneous abatement of N_2O and NO on Pt,Pd,Rh/TiO_2-ZrO_2 and Pt,Pd,Rh/TiO_2-ZrO_2-CeO_2 catalysts

Maria Cristina Campa [a], Giuseppe Fierro [a], Aidan M. Doyle [b], Simonetta Tuti [c], Carlotta Catracchia [d], Daniela Pietrogiacomi [d,e,*]

[a] CNR-Istituto per lo Studio dei Materiali Nanostrutturati, c/o Department of Chemistry, "Sapienza" University of Rome, P.le Aldo Moro, 5 – 00185, Roma, Italy
[b] Department of Natural Sciences, Manchester Metropolitan University, Chester St, Manchester M1 5GD, United Kingdom
[c] Science Department, Roma Tre University, Via della Vasca Navale 79, Rome 00146, Italy
[d] Department of Chemistry, "Sapienza" University of Rome, P.le Aldo Moro, 5 – 00185, Roma, Italy
[e] Research Center for Applied Sciences to the Safeguard of Environment and Cultural Heritage (CIABC), "Sapienza" University of Rome, P.le Aldo Moro 5 – 00185, Rome, Italy

ARTICLE INFO

Keywords:
NO_x and N_2O simultaneous abatement with CH_4
Pt,Pd,Rh on TiO_2-ZrO_2
Pt,Pd,Rh on TiO_2-ZrO_2-CeO_2
SCR reactions
TPR analysis
in situ FTIR characterisation
operando-FTIR analysis

ABSTRACT

Pt,Pd,Rh supported on TiO_2-ZrO_2 and TiO_2-ZrO_2-CeO_2 show a promising catalytic behavior for the simultaneous selective catalytic reduction of NO and N_2O with CH_4 in the presence of O_2 (SCR_{sim}). The nature of the catalytic species and the formation of intermediate species on the catalyst surface were investigated by combining several techniques. The co-existence of fully and partly reduced noble metals are strictly dependent on the O_2/CH_4 ratio in the feed which is crucial for a good catalytic activity. When the O_2/CH_4 ratio is less than 1, NO and N_2O were efficiently and simultaneously reduced with negligible formation of by-products. As the O_2/CH_4 ratio was higher than 1, CH_4 combustion prevailed. The CeO_2 made the catalyst slightly more efficient, likely improving the solid redox properties at the interface between noble metal particles and gaseous reactants. The *operando* FT-IR analysis identified some surface intermediate species involved in the reaction pathways. In the presence of NO, surface nitrite/nitrate species that are strongly adsorbed on the catalysts surface competed with the N_2O adsorption sites. An assay of the SCR_{sim} catalytic behaviour in the presence of water revealed that the catalyst with ceria has a good catalytic activity and stability along tests simulating nearly real conditions.

1. Introduction

The catalytic abatement of nitrogen oxides, i.e. NO_x and N_2O, to less harmful species has been studied for decades and continues to be a topic of research in the pursuit of new and improved systems for emissions abatement [1]. These compounds are by-products of a number of processes e.g. transportation, energy production and bulk chemicals synthesis (nitric acid and adipic acid) and are problematic due to their toxicity (NO) and greenhouse gas potency (N_2O) [2]. It follows that it is of great relevance to develop catalysts which are able to abate simultaneously NO and N_2O. Most studies have focussed on Selective Catalytic Reduction (SCR) of NO, which successfully transforms NO_x to N_2, by reaction with suitable reagents e.g. CH_4, CO, H_2, or NH_3 [3,4]. The most common active components in Three-Way-Converters (TWC) continue to be noble metals, whereby Pt and Pd are active for hydrocarbon oxidation and Rh for NO_x reduction [5–9]. Recently there has been a greater emphasis on N_2O due to its environmental importance and presence in exhaust streams [2,10]. The SCR of NO and the SCR of N_2O has been extensively reported individually, despite the existence of both compounds in exhaust streams. When both gases are present, as in the industrial nitric acid plants, the EnviNOx® process [11] is effective for the abatement of NO_x and N_2O by SCR over two catalytic beds of Fe-zeolite where NO_x is abated by NH_3 and N_2O by CH_x or by NO-assisted decomposition [12,13]. In other studies NO and N_2O were removed sequentially by SCR over Pd-modified perovskites [14] or over dual-bed reactors consisting of Co-ZSM-5 and Pd/Fe-ZSM-5 [15] or In/Al_2O_3 and Ru/Al_2O_3 [16]. In contrast, the simultaneous SCR of NO and N_2O is sparsely discussed in the literature. Some studies were made

* Corresponding author at: Department of Chemistry, "Sapienza" University of Rome, P.le Aldo Moro, 5, Roma 00185, Italy.
E-mail address: daniela.pietrogiacomi@uniroma1.it (D. Pietrogiacomi).

https://doi.org/10.1016/j.surfin.2023.103502
Received 14 July 2023; Received in revised form 5 October 2023; Accepted 7 October 2023
Available online 9 October 2023

over Ag/ZSM-5 [17], Fe-zeolite catalysts [18–22] and over a commercial Bi-Ni-oxide modified V_2O_5-MoO_3/TiO_2 catalyst [23]. We have reported the simultaneous abatement of NO and N_2O in the presence of O_2 with C_3H_6 over ZrO_2 supported CoO_x and FeO_x [24] and over Fe-, Co- and Ni-exchanged MOR catalysts with CH_4 [25], proposing also a reaction pathway using *operando*-FTIR [26].

There is a tendency in the exploration of heterogeneous catalysts to study one catalyst and one reaction in a given experiment. This method is entirely appropriate to infer a correlation between catalyst structure and reactivity, and has brought about a step change in our understanding of catalysis. Of course, 'real' catalysts, e.g. those employed in a TWC washcoat, must be active for a number of different reactions simultaneously and, therefore, require a mixture of supports and catalytically active metals. This adds complexity from (a) the presence of a plurality of catalysts, each of which provides unique catalytic properties analogous to those in their distinct forms, (b) the occurrence of synergistic effects that diverge from those of individual catalysts and (c) the coexistence of several competing reactants each of which interacts differently with the catalysts. This approach of using different mixed supports/catalysts generated promising results in the simultaneous abatement of NO and N_2O with CH_4 as reductant over Pt,Pd,Rh/Al_2O_3-SiO_2 and Pt,Pd,Rh/Al_2O_3-ZrO_2 [27] and has motivated us to continue the study further. CH_4 is an appealing reductant due to a cheap and plentiful supply of natural gas (predominantly CH_4) and being increasingly used as a low carbon substitute for diesel in dual fuel engines for heavy good vehicles (HGVs) [5]. In this work, the activity and selectivity of Pt,Pd,Rh/TiO_2-ZrO_2 and Pt,Pd,Rh/TiO_2-ZrO_2-CeO_2 catalysts in the simultaneous selective catalytic reduction, SCR_{sim}, of NO and N_2O with CH_4 were investigated. Different O_2 feed contents were used as the extent of SCR is dependent on the choice of either lean or rich conditions in the feed [28].

In order to get more insight into the complex mechanism of the SCR_{sim} reaction, the SCR with the single reactant (SCR_{NO}, SCR_{N2O}), as well as the Catalytic Reductions in the absence of O_2 (CR_{sim}, CR_{NO}, CR_{N2O}) were also investigated. For the same purpose, we studied the N_2O decomposition by itself or in the presence of O_2 and NO, and the CH_4 combustion reaction as well.

A combined use of several techniques (XRD, N_2 physisorption, FESEM and H_2-TPR) provided a more comprehensive view of the catalyst characteristics. In order to investigate the surface aspects in more detail, the FTIR spectroscopy has been used. In particular, the interaction of probe molecules (NO or CO) with the catalyst surface under a controlled atmosphere (i.e. *in situ*) was studied by *in situ* FTIR technique. Moreover, the formation of surface intermediates under working condition was investigated by *operando*-FTIR (i.e. spectroscopic measurements carried out in a catalytic reactor in the presence of the reactants mixture and in the reaction temperature range while the catalyst performance is evaluated on-line).

A cross-analysis of the catalytic data with the *operando*-FTIR findings provided new insight into the pathways of the SCR_{sim}, shedding more light on the very complex mechanism of this reaction.

Finally, in order to provide just a first sight of the catalytic behaviour under nearly real conditions, an assay of the catalytic activity was made in the presence of water.

2. Experimental

2.1. Catalysts preparation

Catalysts were prepared by ion-exchange using identical quantities of Pt, Pd and Rh and catalyst treatment (i.e. ultrasound, stirring, filtering, washing, drying and calcination) to that reported previously [27]. The supports were prepared by mixing 1.0 g of TiO_2 (anatase, Millenium) with 1.0 g of ZrO_2 (monoclinic, Sigma 99%) for both the Pt, Pd,Rh/TiO_2-ZrO_2 and Pt,Pd,Rh/TiO_2-ZrO_2-CeO_2 catalysts, in this last preparation being added 0.2 g of CeO_2 (Sigma Aldrich, 99%). The solutions, previously prepared, containing the three noble metals (Pt, Pd, Rh) were added to each of these two supports batches. The resulting suspensions were subjected to ultrasonic treatment, washed, dried and calcined for 4 h in air at 550°C thus giving the final Pt,Pd,Rh/TiO_2-ZrO_2 and Pt,Pd,Rh/TiO_2-ZrO_2-CeO_2 catalysts.

2.2. Catalyst characterization

2.2.1. Chemical, structural and morphological analysis

The quantitative analysis of noble metals was performed by the Wet Chemistry (Te-collection)-ICP-OES methodology in the laboratory of BASF Italia S.p.A., Rome. According to this procedure, the sample is first fused with sodium peroxide, then the melt was dissolved in hot deionized water and acidified with hydrochloric acid until all salts were dissolved. At this point, a solution of tellurium chloride was added, followed by the addition of a solution of stannous chloride with a consequent quantitative coprecipitation of Pd, Pt and Rh. Finally, the tellurium precipitate containing the noble metals was dissolved in aqua regia and the Pd, Pt and Rh measured by ICP-OES.

A Philips PW 1729 diffractometer was used to obtain the X-Ray Diffraction (XRD) patterns under the following experimental conditions: X-ray tube operating at 40 kV and 20 mA, Cu Kα (Ni-filtered) radiation (λ = 1.5406 Å), 10–70° 2θ range (step size 0.02°; step time 1.25 s).

A Micromeritics ASAP 2020 was used for obtaining BET surface areas through nitrogen adsorption/desorption measurements (relative pressure range 0.05-0.30) at -196 °C. Prior to analysis, samples were degassed under vacuum ($p < 10^{-3}$ Pa) for 12 h at 300 °C.

A Field-Emission Scanning Electron Microscope (FESEM) was used to study the morphology of the catalysts either as fresh sample or after catalysis by using an AURIGA Zeiss 405 HR-FESEM instrument which was equipped with an Energy Dispersive X-ray (EDX) Spectroscopy Bruker apparatus for elemental detection.

2.2.2. TPR experiments

The reducibility of the two catalysts was investigated by temperature-programmed reduction (TPR) with H_2 over either the fresh, i.e. as prepared, samples (TPR_{fresh}) or after they underwent catalytic tests (TPR_{catal}). The TPR experiments were carried out with a Thermo Scientific TPDRO1100 apparatus provided with an in-flow system. The consumption of H_2 was measured with a hot wire detector (HWD) calibrated through the reduction of a weighted mass of CuO (purity 99.99% Sigma Aldrich). The catalyst as powder was introduced into a fixed bed tubular reactor in quartz which was placed inside a cylindrical oven whose temperature is regulated by a temperature controller program. At the exit of the reactor, a soda-lime trap was used to remove water formed in the reaction during reduction.

Before starting a TPR run, a weighted amount of a fresh catalyst (0.050–0.100 g) was pretreated at 500°C *in situ* under flowing oxygen (10% O_2/He, v/v) and left at this temperature for 5 min. Then the sample was cooled to room temperature in Ar before starting a TPR run. A mixture of H_2/Ar (5% v/v, 30 ml min^{-1}) passed through the sample and the temperature raised from RT up to 500°C at a heating rate of 10°C min^{-1}, keeping such a final temperature for 1 h. Such experimental operating variables were chosen in order to avoid artefacts along the TPR experiments [29]. The TPR analysis of the catalysts after catalytic tests was made using the same pretreatment *in situ* under flowing oxygen and under the same experimental conditions as for the analogous experiments on the fresh catalysts.

2.2.3. In situ FTIR and operando-FTIR measurements

A Perkin Elmer Frontier spectrometer, equipped with an MCT detector, was used to record FTIR spectra at a resolution of 4 cm^{-1}. The fresh catalysts as powder (20 mg) were pressed (2×10^4 kg cm^{-2}) to obtain self-supporting wafers of about 10 mg cm^{-2}.

The *in situ* characterization was carried out by the adsorption of probe molecules (CO or NO) on samples activated before the

experiments, i.e. (i) evacuation from RT to 500°C, (ii) heating in O_2 at 500°C for 1 h and, in the end, (iii) outgassing at the same temperature for 1 h. For these measurements, a quartz cell provided with KBr windows was used allowing thermal treatments in vacuum or in a controlled atmosphere.

In the *operando*-FTIR experiments, a stainless-steel IR reactor, provided with CaF_2 windows, was used to record spectra on sample wafers up to 500°C under gas stream. The reactor was connected to the same flow apparatus used for catalytic measurements equipped with a gas-chromatograph apparatus for the online analysis of reactants and products. Before the experiments, samples were activated at 500°C in a feed of a 2.5% O_2/He (v/v) mixture and then kept at this temperature for 90 min. Then they were cooled from 500°C to the desired temperature under He flow before being exposed to the catalysis-like feeding mixtures. Spectra were recorded at increasing steps of temperature (from 200 to 500°C). It should be noted that the *operando*-FTIR spectra reported in the figures are difference spectra obtained from the subtraction of the spectra recorded exposing samples to the catalysis-like reactant stream at a given temperature and the spectra coming from a purposely-arranged blank experiment in which the sample was exposed to a He stream at the same temperature.

2.3. Catalytic tests

A flow apparatus at atmospheric pressure was used for the catalytic activity measurements in steady state conditions. The feeding mixtures were obtained by mixing gas flows (pure He, 3% NO in He, 3% N_2O in He, 1.5% CH_4 in He and 10% O_2 in He, all purchased from RIVOIRA and used without further purification) that were independently regulated by mass flow controller-meters (MKS Instruments). In order to guarantee the maximum stream homogeneity, the gas flows were mixed in a glass ampoule before entering the reactor. The catalysts, as powder (ca. 0.150 g), were placed on a sintered frit of a quartz reactor. The analysis of reactants and products was made by a gas-chromatograph (Agilent 7890A GC system) equipped with three columns (Molsieve 5A, for detecting O_2, N_2 and CO; Porapack Q for detecting CO_2 and N_2O; Na_2SO_4-doped alumina for detecting CH_4) and two detectors (TCD and FID). NO was detected by Molsieve 5A only in the absence of O_2 in the reactant stream as the NO_2 formed in the presence of O_2 is not detectable by GC systems. For all the reactants (N_2O, NO, O_2, N_2, CO, CO_2) the GC detection sensitivity is about 10 ppm, with the exception of CH_4 whose detection limit is about 1 ppm.

Before any catalytic run, catalysts were activated by feeding 2.5% O_2/He (v/v) mixture (100 cm^3 min^{-1}) from RT to 500°C and then keeping them isothermally at 500°C for 90 min. In the catalytic runs, the temperature was changed in a random sequence maintaining a constant temperature for at least 30 min (along which three consecutive GC analyses were made to be sure that data did not change) while the catalytic stream continued to flow over the catalyst (total flow rate = 100 cm^3 STP/min and GHSV= 40000 NL kg^{-1} h^{-1}). For the sake of comparison, the reactant concentrations, i.e. N_2O (4000 ppm), NO (4000 ppm), CH_4 (4000 ppm) and O_2 (20000, 5000 or 2500 ppm) (v/v, He as balance), were kept the same in all the reactions investigated. For the catalytic tests in presence of water, a wet feed containing 2.5% v/v of H_2O was obtained using a saturator by bubbling a He stream in the H_2O liquid phase kept at constant temperature (44°C).

Conversions obtained at various W/F ratios (W=sample weight, F=flow rate) indicated that, in our conditions, the reaction is under kinetic control without diffusion effects.

As in detail reported elsewhere [27], percent N_2O, CH_4, total NO or O_2 conversion was calculated as 100 × (molecules consumed)/(molecules injected). Percent NO conversion to N_2 was calculated in SCR_{NO} as 200 × (N_2 produced)/(NO injected) and in SCR_{sim} as 200 × (N_2 produced – N_2O consumed)/(NO injected). Percent CO_2 selectivity was calculated as 100 × (CO_2 formed)/(CO_2+CO molecules formed). The N_2O/CH_4 and O_2/CH_4 ratios were calculated as (N_2O, or O_2, molecules consumed)/(CH_4 molecules consumed).

The C-balance was calculated as (total C atoms inlet)/(total C atoms outlet). The N-balance was calculated as (total N atoms inlet)/(total N atoms outlet). When NO and O_2 are simultaneously present in the mixture, N-balance cannot be calculated as undetectable NO_2 is also formed.

3. Results and discussion

3.1. Catalyst characterization

The analytical content (wt%) of Pt, Pd, and Rh and the BET specific surface areas of the Pt,Pd,Rh/TiO_2-ZrO_2 and Pt,Pd,Rh/TiO_2-ZrO_2-CeO_2 catalysts are reported in Table 1. The specific surface areas of the catalysts correspond well to the mean value of the sum of the surface areas of the two mixed supports.

The XRD patterns of the fresh catalysts shows only the reflections of the anatase TiO_2, monoclinic ZrO_2 and CeO_2 supports (Fig. 1), whose XRD patterns are matching those reported in the reference JCPDS cards (21–1272 for TiO_2 anatase, 37–1484 for monoclinic ZrO_2 and 34–394 for CeO_2). In both fresh catalysts, within sensitivity limits of the technique, no peaks belonging to Pt, Pd and Rh oxide species are detected, suggesting that the diameter of noble metal oxide crystallites, as a mean value, is below ca. 5 nm.

The XRD patterns of both catalysts after catalysis are very similar to those of the fresh materials, but in the case of Pt,Pd,Rh/TiO_2-ZrO_2 a very small and broad peak appears at 2θ=40.2 ° (Fig. 1b) which corresponds to the most intense peak of the Pd metal (Pd(111) [JCPDS card 5-0681]), being the most intense diffraction peak of Pt and Rh metals in different position (39.9° for Pt(111) [JCPDS card 4-0802], and 41.2° for Rh(111) [JCPDS card 5-0685]). Moreover, from the linewidth analysis by using the Scherrer equation, an average crystallite size of Pd of ca. 20 nm is calculated, indicating that some Pd metal crystallites are formed under the catalytic runs.

For the catalysts after catalysis both the line positions and the linewidths of the supports are nearly identical to those for the fresh catalysts, suggesting that, besides the formation of Pd metal phase, no remarkable macroscopic, structural or morphological changes occur in the solid resulting from the catalytic runs.

In the FESEM images and corresponding EDX elemental maps of the Pt,Pd,Rh/TiO_2-ZrO_2 and Pt,Pd,Rh/TiO_2-ZrO_2-CeO_2 as fresh catalysts (Fig. 2a), titania particles (pink coloured) can be distinguished, being characterized by a rougher surface, whereas particles with a more uniform surface correspond to zirconia (green coloured). The CeO_2 support, although not visible in the images due to its very low amount, can be

Table 1
Pt, Pd and Rh content, specific surface areas and TPR quantitative analysis.

Sample Name	Pd wt%	Pt wt%	Rh wt%	S_{BET}[a] (m^2 g^{-1})	H_2 uptake (mmol g^{-1})		
					theor[b]	exper. (fresh catalyst)	exper. (after catalysis)
TiO_2				103			
ZrO_2				35			
Pt,Pd, Rh/ TiO_2-ZrO_2	0.66	0.85	0.82	49	0.22	0.20	0.14
Pt,Pd, Rh/ TiO_2-ZrO_2-CeO_2	0.65	0.84	0.98	64	0.25	0.23	0.18

[a] S_{BET} = BET specific surface areas (m^2 g^{-1})
[b] The theoretical H_2 consumption was calculated under the hypothesis that PdO, PtO and Rh_2O_3 were the oxide-like species formed after calcination at 500°C

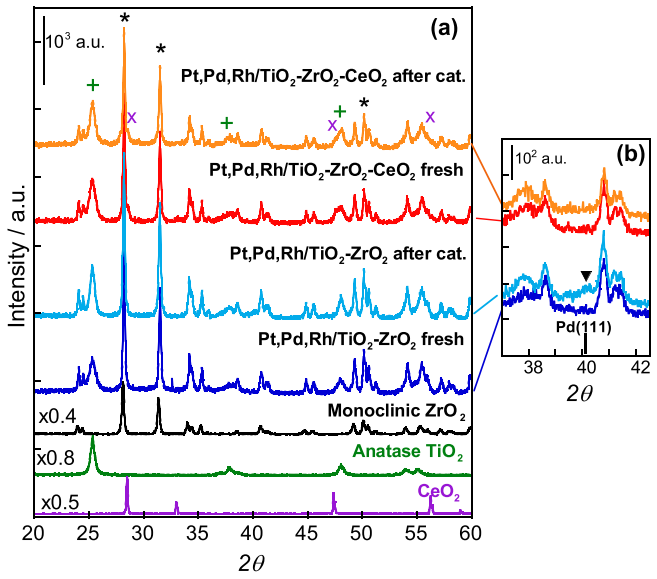

Fig. 1. XRD patterns of Pt,Pd,Rh/TiO_2-ZrO_2 and Pt,Pd,Rh/TiO_2-ZrO_2-CeO_2 catalysts as fresh samples or after catalysis (section a). The XRD patterns of monoclinic ZrO_2 (*), anatase TiO_2 (+), and CeO_2 (×) supports are also reported as reference. The marks on the XRD patterns of the catalysts refer to the position of the three most intense lines of the supports. Section b shows the magnification of the region in which the most intense peak of Pt, Pd, Rh metal phases are expected, showing the Pd(111) reflection position. From the FWHM value of the Pd peak, the Pd mean crystallite diameter (reported in the text) was calculated by the Scherrer equation ($d = K\lambda/\beta\cos\theta$).

identified in the EDX elemental maps (see Fig. 2a). The noble metal oxides, detected by EDX, were not distinguished in the FESEM images, probably because they are dispersed on the support as very small nanoparticles, this being supported also by XRD analysis which did not reveal any noble metal oxides phases.

In the catalysts after catalysis (Fig. 2b), if compared to the fresh material, the FESEM images show noble metal nanoparticles which are heterogeneous in size (from ca. 2 to ca. 50 nm), lying on the supports and characterised by rounded morphology. These noble metal nanoparticles are made by aggregates of small crystallite, which only in the case of Pd in Pt,Pd,Rh/TiO_2-ZrO_2 catalyst are detected by XRD (vide supra), which is able to reveal crystallites larger than ca. 5 nm. In the EDX elemental maps of such crystallite aggregates, the Pd, Pt and Rh escaped the detection as single particles, showing signals for each noble metal spread all over the scanned area (insets in Fig. 2b).

After catalysis in the presence of H_2O (Fig. 2c), a larger heterogeneity in size of noble metal nanoparticles is observed and a detectable aggregation of Pd occurred. Indeed, Pd metal is now distinguished by EDX analysis in the form of aggregates reaching ca. 100 nm in size (see Fig. 2c, inset EDX analysis), suggesting that Pd is more sensitive with respect to Pt and Rh to be aggregated in the presence of H_2O.

3.2. TPR analysis

The H_2-TPR profiles of the fresh Pt,Pd,Rh/TiO_2-ZrO_2 and Pt,Pd,Rh/TiO_2-ZrO_2-CeO_2 catalysts are both characterized by a rather complex pattern which, with some differences, is still present in the reduction profiles of the catalysts after the catalytic runs (Fig. 3a and b).

The common features evident in the TPR profiles of both catalysts either as fresh materials or after catalysis are represented by a wide band whose intensity, as a whole, is continuously increasing with increasing temperature (see Fig. 3). In such a wide band some peaks can be distinguished, less resolved in the lower temperature side (from RT up to about 280°C), with the exception of the Pt,Pd,Rh/TiO_2-ZrO_2-CeO_2 catalyst in which after catalysis the poor resolved peaks became more evident (see Fig. 3b). For both catalysts, regardless their initial state (fresh or after catalysis), a well-defined and larger peak appeared in the high temperature side (from 280 to 500°C). Such a complex shape can be due to the gradual occurring of the reduction of the PdO_x, PtO_x and Rh_xO_y oxide-like species as well as to possible overlapping of these reduction processes. A further complication is represented by two other factors: (i) the influence of the supports, in particular CeO_2, that very likely play a role in these processes through a noble metal oxide-support interaction, or a synergy between CeO_2, ZrO_2 and TiO_2 as recently reported in literature [30]; (ii) the formation of metals (Pd and Pt in the first stage) which, as it is well known, can activate the H_2 molecule thus enhancing the overall reduction process.

For both the Pt,Pd,Rh/TiO_2-ZrO_2 and Pt,Pd,Rh/TiO_2-ZrO_2-CeO_2 catalysts, a negative peak at ca. 70°C can be attributed to the decomposition of some Pd-hydride species (β-PdH_x) which can give rise to the desorption of H_2 (thus enriching the reducing stream) chemisorbed on the Pd surface or adsorbed in the bulk of metal Pd particles [31–33]. In agreement with a mechanism already described [31], it can be suggested that PdO_x-like species, formed after calcination at 550°C on the TiO_2-ZrO_2 and TiO_2-ZrO_2-CeO_2 supports, are reacting first with H_2 even at room temperature forming β-PdH_x species. Interestingly, such a negative peak is always present regardless of the catalyst composition and its initial state (fresh or after catalysis), suggesting that the formation of β-PdH_x species at low temperature is not influenced by the catalyst history.

In the lower temperature region (from 50 up to ca. 180°C), besides the negative peak, a wide band characterized by poorly resolved components can be observed which, as a whole, can be due to the reduction of isolated or well dispersed PdO_x, PtO_x and Rh_xO_y species [31,34,35].

In the middle temperature region (from ca. 180°C up to ca. 265°C), the H_2 detector signal is still slowly increasing, although in the case of the Pt,Pd,Rh/TiO_2-ZrO_2-CeO_2 catalyst after catalysis (see Fig 3b) it decreased a little but just to form a valley after a peak and then it continued to increase as in the other cases never coming back to zero. It follows that, in the middle region temperature, the H_2 uptake did not stop but it was still in progress, meaning that any reduction, of a single or multiple species, continued to occur and, as a whole, proceeded slowly as a continuum. It can be suggested, in agreement with literature [34,35], that the reduction of supported PtO_x and Rh_xO_y species can mainly occur along this range of temperatures, as the Pd oxide-like species are prevalently reduced in the lower temperature range.

In the higher temperature region (from 265°C up to 500°C), a large and clearly defined peak at ca. 370°C was present in the TPR profiles of both catalysts either as fresh material or after catalysis (see Fig. 3). According to literature [35], such a large peak at ca. 375°C can be mainly due to Rh_xO_y species which are more strongly interacting with the supports. However, it cannot be excluded that also some residual PtO_x or even PdO_x species more strongly interacting with the support can be reduced at higher temperature, thus contributing to the peak at ca. 375°C. In spite of the drift of the baseline, which seems to be a characteristic of the TPR profiles of supported noble metals systems [32, 36], an estimate of the total H_2 consumption was made and it was in good agreement with the theoretical H_2 consumption under the hypothesis that PdO, PtO and Rh_2O_3 were the oxide-like species formed after calcination at 500°C (see Table 1). On the basis of the total H_2 consumption and in agreement with the results reported in literature, it can be reasonably suggested that, in both Pt,Pd,Rh/TiO_2-ZrO_2 and Pt,Pd,Rh/TiO_2-ZrO_2-CeO_2 catalysts, the noble metals were fully reduced to the metal state at the end of the TPR runs, at least under our experimental conditions.

However, besides the common features described above, the TPR profiles of both catalysts after the catalytic runs evidenced also some differences (see Fig. 3). In particular, a shift from ca. 370°C to ca. 400°C of the largest peak present in the higher temperature side was evident, very likely related to a strengthening of the Rh_xO_y-support interaction.

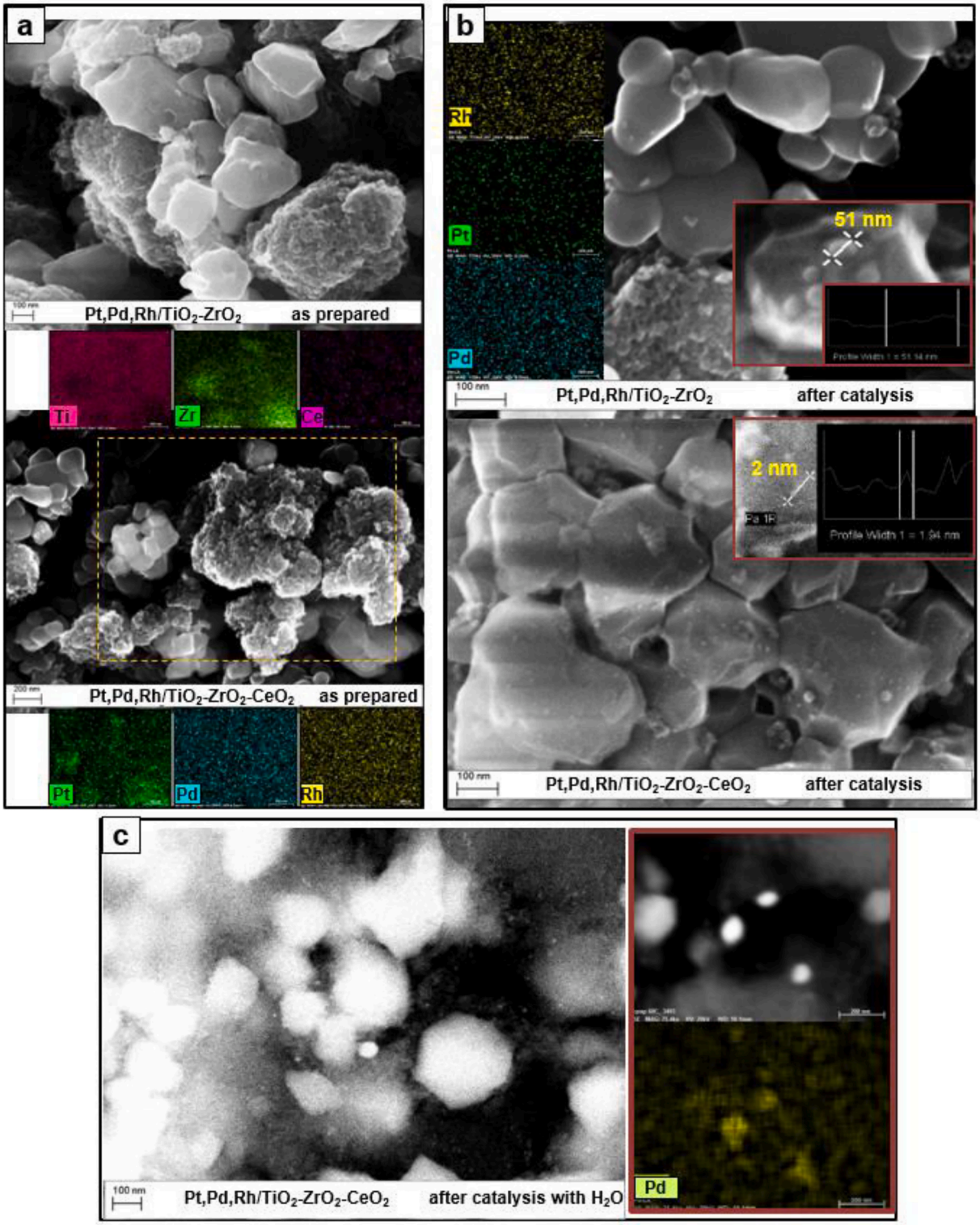

Fig. 2. FESEM images of Pt,Pd,Rh/TiO_2-ZrO_2 and Pt,Pd,Rh/TiO_2-ZrO_2-CeO_2 catalysts as prepared (section a, In-Lens detector), after the catalytic tests (section b, In-Lens detector) and after catalysis in the presence of H_2O (section c, Back Scattering detector). The EDX elemental maps (coloured images) are reported in section a (referring to the dotted marked area) for Zr, Ti, Ce, Pt, Pd and Rh, in section b for Pt, Pd and Rh, and in section c for Pd.

This effect suggested that structural changes of the Rh species occurred in consequence of the redox cycles along the SCR_{sim} reaction. Indeed, such a dynamic redox behavior of Rh species has been recently reported for a Rh/Al_2O_3 catalyst in a very elegant paper showing that structural changes of Rh species due to complex reduction/oxidation processes of oxide-like and metal-like Rh particles can occur under a reactant stream simulating a Three-Way Catalytic Reaction [9]. Additionally, the rising up of a shoulder at ca. 300°C for Pt,Pd,Rh/TiO_2-ZrO_2 catalyst and of a better defined peak at ca. 225°C for the Pt,Pd,Rh/TiO_2-ZrO_2-CeO_2 catalyst were evident. These effects can be related to some changes in size and/or morphology of the Pd and Pt oxide-like particles during the catalytic reactions and/or to a different interaction with the support.

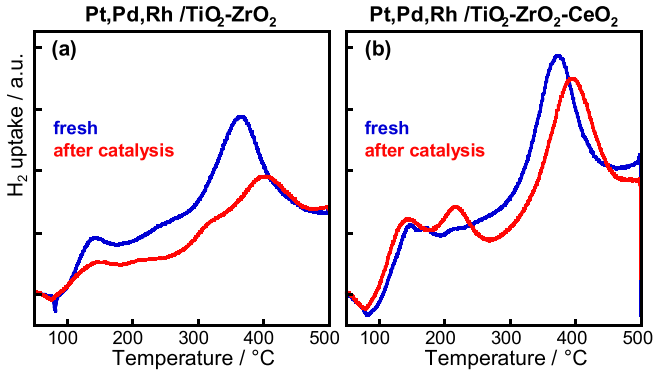

Fig. 3. TPR profiles of (section a) Pt,Pd,Rh/TiO_2-ZrO_2 and (section b) Pt,Pd,Rh/TiO_2-ZrO_2-CeO_2 catalysts, either as fresh material or after the catalytic runs.

Moreover, the TPR quantitative analysis of the catalysts after catalytic runs suggests that the oxidizing pre-treatment did not convert the catalysts to their initial fully oxidized state. These findings, as a whole, suggest that, along the catalytic runs, some changes of the nature of the catalysts occurred.

3.3. In situ FTIR analysis of the surface species using NO or CO as probe molecules

FTIR spectra of both Pt,Pd,Rh/TiO_2-ZrO_2 and Pt,Pd,Rh/TiO_2-ZrO_2-CeO_2 catalysts, recorded at room temperature upon adsorption of NO at increasing pressure (0.5≤ NO≤ 100 Torr), showed a progressive increase of various peaks in the frequency range 1950–1700 cm^{-1} (Fig. 4a). Additionally, small contributions at about 2250 cm^{-1} and in the 1620–1550 cm^{-1} region and a negative peak at 1356 cm^{-1}, coupled to a positive peak at 1345 cm^{-1}, appeared in the spectra. Peaks in the range 1950–1700 cm^{-1} can be attributed to nitrosyls adsorbed on the various atomic species present on the catalyst surface. At low NO pressure values (<1 Torr), the peaks appearing first were those in the range 1835–1700 cm^{-1}, which have been assigned to neutral nitrosyls formed on cationic or metal sites (like Pd^{n+}, Rh^{+}, Pt^{0} and Rh^{0}) [37–40]. The most intense peak at about 1800 cm^{-1} and the couple of peaks at 1830 and 1740 cm^{-1} are usually ascribed to Rh-NO and Rh-$(NO)_2$ gem-dinitrosyls, respectively [37], thus suggesting that, among noble-metals, Rh exposed sites yielded the most stable nitrosyl complexes and has at least two coordinative unsaturations. At intermediate pressure values (<10 Torr), the peak at ca. 1940 cm^{-1}, assigned to Pt^{2+}-NO [37], and the peak at 1914 cm^{-1}, attributed to positively charged Rh^{0}-NO^{+} [38,39], increased. At the higher pressure values (≤100 Torr), the peak at 1901 cm^{-1} can be assigned to a labile Ti^{4+}-NO species which markedly increased and then disappeared after outgassing. As a whole, such a plethora of peaks are clearly indicating that many coordinatively unsaturated sites (CUS) existed on the surface of noble metal particles and that Rh yields the strongest interaction with NO.

The contributions at 2250 cm^{-1} and in the 1620–1550 cm^{-1} region (see Fig. 4a) were due to adsorbed N_2O and adsorbed nitrite/nitrate species, respectively, originating from NO disproportion on the oxide surface [40]. The amount of such species was rather large in the CeO_2-containing Pt,Pd,Rh/TiO_2-ZrO_2-CeO_2 catalyst (see Fig. 4a), for which more defined bands of bidentate nitrate species (about 1570, 1330 and 1180 cm^{-1} [40]) appeared. This result suggests that CeO_2 enhanced the interface reactivity, promoting the NO disproportion on its reactive surface O sites. Finally, the coupled negative/positive peaks arose from the red-shift of an adsorption mode, probably of a surface termination, as a titanyl-like Ti=O species [41], interacting with an adjacent electron-withdrawing species, as the adsorbed nitrites/nitrates. A similar red-shift has been already reported for the stretching mode of S=O in sulphate species covalently bonded to the surface of oxides [42].

In the case of CO adsorption at RT (Fig. 4b), bands in the carbonyl region of 2220–1950 cm^{-1} and in the carbonates region below 1650 cm^{-1} appeared in the spectra of both Pt,Pd,Rh/TiO_2-ZrO_2 and Pt,Pd,Rh/TiO_2-ZrO_2-CeO_2 catalysts, the intensity of all bands increasing with increasing CO pressure. In particular, the peaks in the range 2205–2185 cm^{-1}, assigned to labile carbonyls (bonded through σ-donation) on TiO_2 and ZrO_2 supports, are the most sensitive to CO pressure, markedly increasing as CO pressure increased and disappearing on evacuation (dotted lines in Fig. 4b). The adsorption on TiO_2 typically occurred on two types of CUS, α-Ti^{4+} and β-Ti^{4+}, yielding peaks at about 2205 and 2190 cm^{-1} [43], while the adsorption on Zr^{4+} gave rise to a band at 2200–2190 cm^{-1}, red-shifting as CO pressure increased [44]. The band envelope at lower wavenumbers (2190–2000 cm^{-1} region), progressively increasing as CO pressure increased, are due to more stable carbonyls (bonded through σ-donation reinforced by π-back donation) as, differently from carbonyls on the support sites, they are nearly unaffected by evacuation. The envelope consisted of several peaks (at 2180, 2160, 2136, 2100, 2090, 2075, and 2036 cm^{-1}) assignable to different types of (i) linear carbonyls on oxidised (Pt^{2+}, Pd^{n+} and Rh^{+}, peaks above 2100 cm^{-1}) and on reduced (Pt^{0}, Pd^{0} and Rh^{0}, peaks below 2100

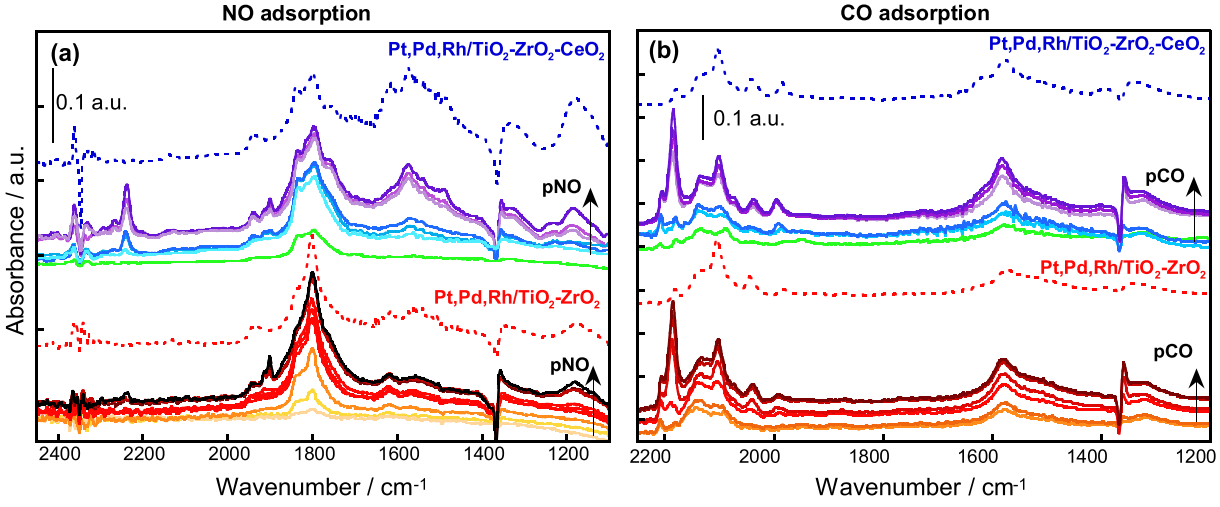

Fig. 4. FTIR spectra, gas subtracted, after (section a) NO and (section b) CO adsorption at RT on activated Pt,Pd,Rh/TiO_2-ZrO_2 and Pt,Pd,Rh/TiO_2-ZrO_2-CeO_2 catalysts at increasing equilibrium pressure (from 0.050 to 100 Torr) and after evacuation for 5 min (dotted lines).

cm^{-1}) noble-metal sites and of (ii) bridged carbonyls on reduced sites (about 1998 cm^{-1}) [37,45-48]. At the higher CO pressure, the bands at 2100 and 2036 cm^{-1} become predominant in the envelope and have been assigned to a gem-dicarbonyl $Rh^{+}(CO)_2$ complex (ν_{asym} and ν_{sym}) on isolated Rh^{+} sites [49], confirming that the degree of coordinative unsaturation for the Rh exposed surface sites is at least two. Bands typical of carbonates (1580, 1320 and 1050 cm^{-1} [50]) and the coupled negative/positive peaks (1370 and 1360 cm^{-1}) appeared in the spectral region below 1650 cm^{-1} (see Fig. 4b). It should be noted that the simultaneous formation of carbonates and of carbonyls formed on (fully or partially) reduced noble-metal atoms indicated a surface reaction in which surface noble-metal ions are reduced by CO with a consequent formation of CO_2 that yielded adsorbed carbonates. This process occurred promptly as CO contacted the samples even at low pressure, pointing to the presence of highly reactive surface oxygen species that are available for interface redox processes even at room temperature. The coupled negative/positive peaks, already observed after NO adsorption (vide supra), were in this case possibly due to the interaction of the previously suggested surface Ti=O species with an adjacent adsorbed electron-withdrawing carbonate.

In order to shed more light on the surface redox properties, CO was used simultaneously as a reducing agent and as a probe molecule. To this purpose, the catalysts were first heated at different temperatures (from 100 to 300°C) in CO at a fixed pressure (ca. 100 Torr). After treatment at each temperature, the spectrum was recorded at RT after cooling in CO.

In the case of the Pt,Pd,Rh/TiO_2-ZrO_2 catalyst (Fig. 5a), upon heating in CO some remarkable changes in the spectra occurred in the noble-metal carbonyl region (2180–1990 cm^{-1}), while bands from carbonyls

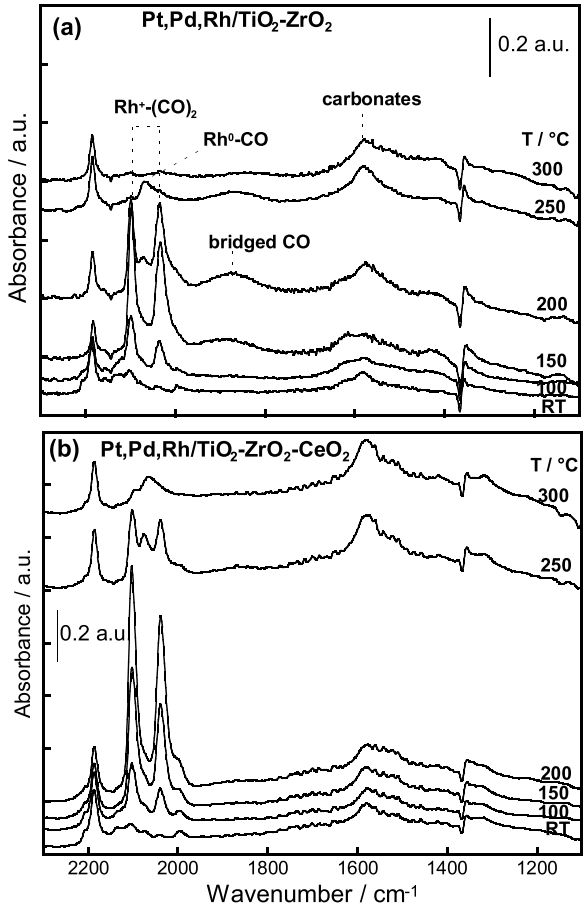

Fig. 5. *In situ* FTIR spectra after CO adsorption at room temperature (RT) and subsequent heating in CO at increasing temperature up to 300°C (stepwise of 50°C) on activated (section a) Pt,Pd,Rh/TiO_2-ZrO_2 and (section b) Pt,Pd,Rh/TiO_2-ZrO_2-CeO_2 catalysts.

on the support sites remained practically the same. In particular, heating in CO up to 150°C, the intensity of weak bands from oxidized noble-metal carbonyls (2180–2100 cm^{-1}) decreased, whereas the bands of reduced noble-metal carbonyls (2100–1990 cm^{-1}) and those of Rh^{+}-$(CO)_2$ dicarbonyls (2100 and 2036 cm^{-1} [49]) increased. It should be noted that Rh^{+}-$(CO)_2$ dicarbonyls reached their maximum intensity at 150°C. This trend, together with the increase of carbonate bands intensity (around 1600 cm^{-1} [50]), proves that an additional fraction of the surface noble-metal ions was progressively reduced as the temperature increased. This is also supported by the formation of bridged carbonyl species (broad band at about 1880 cm^{-1}), which typically formed on metal species. On increasing the temperature up to 250°C, the Rh^{+}-$(CO)_2$ dicarbonyl bands progressively decreased while a band at about 2050 cm^{-1}, likely ascribed to Rh^{0}-CO species [51], increased. At 300°C carbonyls on noble metal species almost disappeared, suggesting that dissociative chemisorption of CO occurred poisoning the adsorbing sites.

For the sample Pt,Pd,Rh/TiO_2-ZrO_2-CeO_2, although a similar trend upon CO thermal treatment occurred, some important differences can be noticed with respect to the Pt,Pd,Rh/TiO_2-ZrO_2 (Fig. 5b): (i) the Rh^{+}-$(CO)_2$ dicarbonyl bands reached the maximum intensity at higher temperature (200°C vs. 150°C), (ii) Rh^{0}-CO formation was evidenced at higher temperature (250°C vs. 200°C), and (iii) bridged carbonyls on metal species (1880 cm^{-1}) formed in a negligible amount. All these findings suggested that the Rh_xO_y species were less reducible in the presence of CeO_2.

As a whole, from these findings it can be suggested that the surface species exposed on the surface of the noble metal oxide-like particles are characterized by a different reducibility. Among the exposed surface species, the Rh_xO_y are likely the least reducible ones, being stabilised as Rh^{+}. These conclusions are in agreement with the analysis of the TPR results showing that the Rh_xO_y species reduced at higher temperature while the PdO_x and PtO_x oxide-like species reduced at lower temperatures (see Fig. 3), the reduction of PdO_x occurring first (vide supra). Also the FTIR evidenced that Rh_xO_y species are less reducible in the presence of CeO_2, in very good agreement with the TPR results.

3.4. Catalytic activity

3.4.1. Simultaneous abatement of NO and N_2O with CH_4 in presence (SCR_{sim}) or absence (CR_{sim}) of O_2

The O_2 content in the NO+N_2O+CH_4+O_2 mixture (SCR_{sim}) markedly affected the activity and selectivity of the Pt,Pd,Rh/TiO_2-ZrO_2 and Pt,Pd,Rh/TiO_2-ZrO_2-CeO_2 catalysts for the simultaneous abatement of NO and N_2O with CH_4. When the O_2 content was 2500 ppm, a good activity and a good CO_2 selectivity (>90% over the entire temperature range) for the SCR_{sim} were found on both catalysts (Fig. 6). Indeed, in such conditions they were effective for the conversion of NO and N_2O to N_2 that sharply increased as the temperature increased and reached their maximum value (about 90% and about 100%, respectively) at 425°C on Pt,Pd,Rh/TiO_2-ZrO_2 catalyst and at 400°C on Pt,Pd,Rh/TiO_2-ZrO_2-CeO_2 catalyst (see Fig. 6). Such a small difference of temperature may be ascribed to the presence of ceria that, due to its well-known ability to give rise to oxygen vacancies and reactive oxygen species [30], can improve the redox properties of the Pt,Pd,Rh/TiO_2-ZrO_2-CeO_2 catalyst, and consequently, the catalytic activity. In the case of NO, above ca. 400°C the conversion decreased to some extent forming a depressed curve with a minimum, which was more evident for Pt,Pd,Rh/TiO_2-ZrO_2-CeO_2 (70%, see Fig. 6), suggesting the formation of by-products. Since the C-balance remained at 100%, the eventually formed species are only N-containing by-products (like NH_3).

When water (2.5% v/v) was added to the NO+N_2O+CH_4+O_2 mixture to simulate nearly real conditions, the catalytic behaviour for the ceria-containing catalyst was not negatively but positively affected (Fig. 6c). In particular, at 500°C and 450°C the N_2O and CH_4 conversions remained at 100% while the NO conversion and the CO_2 selectivity were

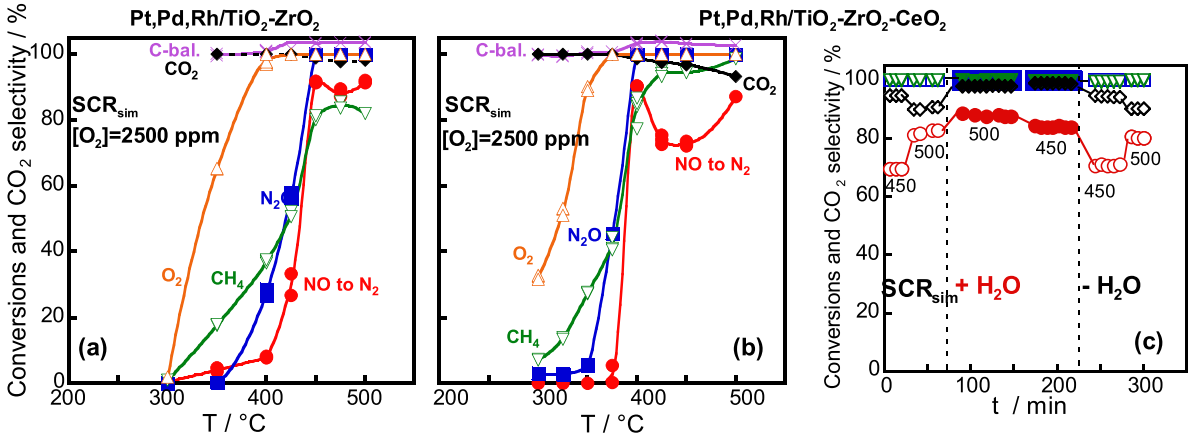

Fig. 6. The activity for simultaneous abatement of NO and N_2O with CH_4 in the presence of O_2 as a function of temperature on (section a) Pt,Pd,Rh/TiO_2-ZrO_2 and (section b) Pt,Pd,Rh/TiO_2-ZrO_2-CeO_2 under dry feed. For the last sample, the activity under dry (open symbols) or wet feed (containing 2.5 % v/v of water vapour, solid symbols) was reported as a function of exposure time to the feed (section c). NO to N_2 (●), N_2O (■), CH_4 (▽) and O_2 (△) conversions, CO_2 selectivity (◆), C-balance (×) as a function of temperature or time. Reactants concentration: [N_2O]=[NO]=[CH_4]=4000 ppm, [O_2]=2500 ppm, [H_2O]=25000 ppm (if present); total flow rate=100 cm^3 STP/min, He as balance.

even better in the presence of water. Moreover, when water was removed from the stream, the Pt,Pd,Rh/TiO_2-ZrO_2-CeO_2 catalyst went back to the original catalytic activity (see Fig. 6c), suggesting that in the presence of water the active sites were preserved sustaining a catalytic behaviour at least as good as shown before water was added. This is somewhat expected being an usual behaviour of the TWC's reported in literature as outlined in a study of the three-way behaviour of platinum-alumina-ceria catalysts [52]. In this paper the increase of NO abatement activity when water was added to an exhaust-simulating feed stream has been justified by two factors: (i) the occurrence of the water-gas shift reaction, enhanced by cerium oxide, making weaker the CO adsorption on metal platinum active sites and, as a consequence, decreasing its self-poisoning effect; (ii) NO can react also with the products of the water-gas shift reaction.

When O_2 was absent from the mixture (i.e. NO+N_2O+CH_4, CR_{sim}), both catalysts showed almost the same catalytic behaviour. In Fig. 7a the results for the Pt,Pd,Rh/TiO_2-ZrO_2 catalyst are presented as a representative sample. If compared to the SCR_{sim} reaction with 2500 ppm of O_2, the CR_{sim} was slightly less effective due to selectivity issues. Indeed, the N_2O and the total NO conversions, starting at about 300°C together with the CH_4 conversion, were about 100% above 400°C, but the NO conversion to N_2 was lower, being about 80% in the same temperature range (Fig. 7a). Moreover, the CO_2 selectivity decreased at 85% as the temperature increased to 500°C due to CO formation. It should be noted that, above ca. 375°C, while the C-balance was always 100%, the N-balance was nearly 90%, confirming that, as for the SCR_{sim} (vide supra), a small amount of only N-containing by-products (like NH_3) was formed.

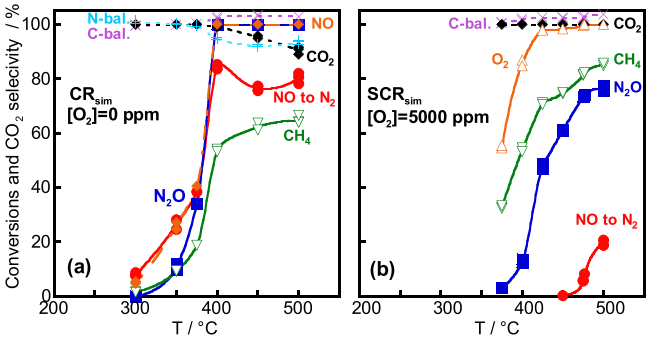

Fig. 7. Simultaneous abatement of NO and N_2O with CH_4 in the absence (CR_{sim}, section a) and in the presence of O_2 (SCR_{sim}, section b) on Pt,Pd,Rh/TiO_2-ZrO_2. NO to N_2 (●), N_2O (■), CH_4 (▽), O_2 (△) conversions, CO_2 selectivity (◆), C-balance (×) and N-balance (+) as a function of temperature. Reactants concentration: [N_2O]=[NO]=[CH_4]=4000 ppm, [O_2]=0 or 5000 ppm (total flow rate=100 cm^3 STP/min, He as balance).

By contrast, when O_2 in the mixture was 5000 (or 10000 ppm), the SCR_{sim} was not effective over the entire range of temperature explored (250-500°C). In particular, at 5000 ppm of O_2, the N_2O conversion reached ca. 80% only at 500°C and the NO conversion to N_2 was at most 20% at the same temperature (see Fig. 7b). On increasing the amount of O_2 to 10000 ppm, the situation became worse because, while the N_2O conversion remained similar, the NO conversion became negligible. Literature data supported our results on the effect of the O_2 content in the reactant mixture. Indeed a similar trend was observed for the NO conversion on Rh/ZrO_2 [53] as well as on Ce–Zr promoted Pd–Rh/Al_2O_3 catalysts [28], showing that the NO conversion decreased monotonically on increasing air to fuel (A/F) ratio.

It is relevant to note that the CH_4 conversion in SCR_{sim}, either at O_2 content of 2500 or 5000 ppm, started on both catalysts at ca. 250°C together with the conversion of O_2, well before the temperature range at which the N_2O and NO started to be converted (about 350-375°C, see Figs. 6 and 7b). This finding suggests that from 250°C up to 350-375°C only the competitive CH_4 combustion occurred. It should be pointed out that, even at the lowest O_2 amount (2500 ppm) at which the best activity and selectivity were found, N_2O and NO started to be converted only when O_2 was almost completely consumed by CH_4. After this point, the remaining CH_4 continued to react with NO and N_2O until they were almost completely converted above 400°C (see Fig. 6). The presence of O_2 in the feed is important in order to guarantee the CO_2 selectivity at a value of 100% on Pt,Pd,Rh/TiO_2-ZrO_2 and at values higher than 90% on Pt,Pd,Rh/TiO_2-ZrO_2-CeO_2 over the entire temperature range (see Fig. 6).

3.4.2. *SCR_{N2O}, SCR_{NO}, CR_{N2O}, CR_{NO} and related reactions*

In order to have more insight into the catalytic behaviour of both Pt,Pd,Rh/TiO_2-ZrO_2 and Pt,Pd,Rh/TiO_2-ZrO_2-CeO_2 catalysts for the SCR_{sim} reaction, the activity for the main competitive side-reaction, i.e. CH_4 combustion (CH_4+O_2), was investigated. Moreover, for the same purpose, the separate abatement reactions of NO or N_2O, either in the absence (CR_{NO}, CR_{N2O}) or in the presence of different amount of O_2 (SCR_{NO}, SCR_{N2O}), as well as the N_2O decomposition, by itself or in the presence of O_2 or NO, were also investigated.

CH_4 combustion. Both catalysts were very active for the CH_4 combustion at the O_2 content of 2500 ppm, the value at which the best performance for SCR_{sim} was observed. The light-off temperature of the

CH_4 combustion was at ca. 200°C. On increasing temperature, O_2 conversion became 100% already at 325°C while the CH_4 conversion was still increasing (Fig. 8a). Moreover, above 350°C on both catalysts the CO_2 selectivity markedly decreased, with only CO and CO_2 observed as reaction products (Fig. 8b). It should be noted that, at this low amount of O_2 in the mixture (much less than the stoichiometric value for total combustion), the decrease of the CO_2 selectivity, the simultaneous decrease of the O_2/CH_4 values and the full C-balance (Fig. 8b) occurred all together. How can this combination of factors be explained? A reasonable explanation, supported by literature, can be that some syngas ($CO+H_2$) was formed through CH_4 partial oxidation, in agreement with the well-recognised activity of noble metals for this reaction [51]. The evidence found that the CH_4 combustion light-off occurred at 200°C, a temperature at which in the SCR_{sim} with O_2 at 2500 ppm N_2O and NO were both not yet converted while the CH_4 and O_2 conversions already occurred (see Fig. 6), is confirming that in the lower temperature range of the SCR_{sim} the competitive CH_4 combustion took place.

As anticipated in our previous work [27], Pd and Pt are very likely the main species responsible for total oxidation of methane, acting possibly in a synergism [8]. In particular, Pd, or the Pd-PdO_x interface, is considered to be one of the most active materials for this reaction in lean combustion conditions [54,55], also in the presence of NO [56]. The combustion activity has been directly related to the PdO reducibility strongly affected by the support that influenced the Pd-O bond strength [55]. Moreover, it has been reported that the Pd activity increases with the increase of the oxygen vacancies on the PdO surface [57]. Since, as evidenced by the TPR results, the Pd species are the most easily reducible metal ion species in the catalysts, it is reasonable that Pd metal, likely together with Pt, is formed by reduction with CH_4 not only during combustion but also along the SCR_{sim}, as confirmed by the XRD analysis (vide supra).

SCR_{NO} and CR_{NO} reactions. On both Pt,Pd,Rh/TiO_2-ZrO_2 and Pt,Pd,Rh/TiO_2-ZrO_2-CeO_2 catalysts, the separate NO abatement in the presence of O_2 (SCR_{NO}) at 2500 ppm, at which the best performance for SCR_{sim} was observed, showed a behaviour similar to that found in absence of O_2 (CR_{NO}). However, some differences can be noticed.

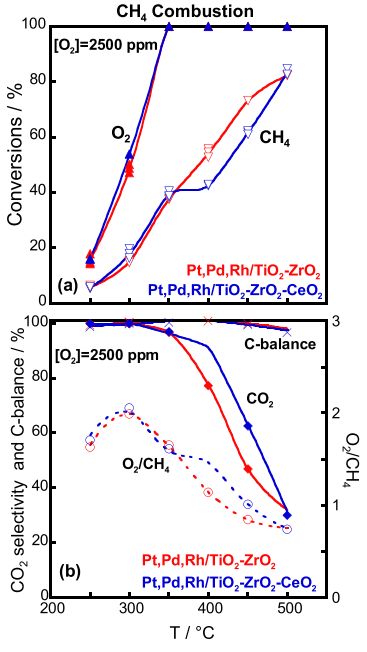

Fig. 8. CH_4 combustion on Pt,Pd,Rh/TiO_2-ZrO_2 and Pt,Pd,Rh/TiO_2-ZrO_2-CeO_2. CH_4 (▽) and O_2 (▲) conversions (section a), CO_2 selectivity (◆), C-balance (×) and O_2/CH_4 ratio (O) as a function of temperature (section b). Reactants concentration: [CH_4]=4000 ppm, [O_2]= 2500 ppm (total flow rate=100 cm^3 STP/min, He as balance).

Although both catalysts were active for NO reduction by CH_4, with a similar activity either for the SCR_{NO} (Fig. 9a and b) or CR_{NO} (Fig. 9c and d), a remarkable difference was observed for the light-off temperature. It was 350°C for SCR_{NO}, with a very steep increase of the NO conversion to N_2 from 0 to 100% in a very short range of temperature (see Fig. 9a) occurring when O_2 was completely consumed by CH_4. On the other hand, the light-off temperature for the CR_{NO} occurred at much lower temperature (250°C) with a gradual increase of the NO conversion to N_2 which became 100% at the same temperature observed for SCR_{NO} (350°C, Fig. 9c). The difference in the light-off temperature in the separate NO abatement reactions is confirming the inhibiting effect of O_2 on the NO conversion already observed in the SCR_{sim}.

However, above 350°C the NO conversion to N_2 decreased going through a minimum in both SCR_{NO} and CR_{NO} reactions, thus indicating the formation of some N-containing by-products. Since the C-balance was nearly 100% in the whole temperature range explored, the N-containing by-products are not containing C species (likely NH_3, since N_2O was never detected). On the other hand, CH_4 conversion, starting at 250°C for both reactions, increased with increasing temperature all along the temperature range (Fig. 9a and c). Above 350°C, side-reactions consuming CH_4 but yielding CO occurred as proved by the trend of the CO_2 selectivity. In particular, CO_2 selectivity decreased from 100% to 70% at 500°C in the case of SCR_{NO}, while it markedly decreased from 100% to 20% for CR_{NO} (Fig. 9d). It can be noticed that the presence of O_2, although having a negative effect due to the inhibition of the NO conversion light-off, plays a positive role improving the CO_2 selectivity.

Both these effects were still observed to a higher extent in the SCR_{NO} on increasing the O_2 amount from 2500 to 5000 and 10000 ppm. If compared to the SCR_{NO} at 2500 ppm of O_2, the light-off temperature shifted to higher values for O_2 at 5000 ppm (about 375°C) and even NO conversion never occurred at 10000 ppm (Supplementary Fig. 1). On the other hand, the CO_2 selectivity remarkably improved, being almost

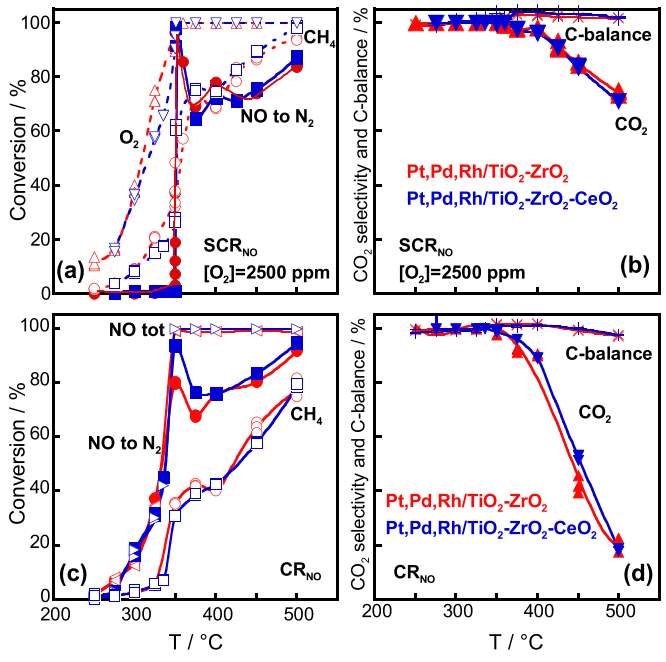

Fig. 9. SCR_{NO} (sections a and b) and CR_{NO} (sections c and d) reactions on Pt,Pd, Rh/TiO_2-ZrO_2 (red symbols) and Pt,Pd,Rh/TiO_2-ZrO_2-CeO_2 (blue symbols) catalysts. NO to N_2 (●,■), total NO (◁,▷), CH_4 (○,□) and O_2 (△,▽) conversions as a function of temperature (sections a and c); CO_2 selectivity (▲,▼), and C-balance (×,+) as a function of temperature (sections b and d). The first symbols in parentheses refer to Pt,Pd,Rh/TiO_2-ZrO_2, the second ones to Pt,Pd, Rh/TiO_2-ZrO_2-CeO_2. Reactants concentration: [NO]=[CH_4]=4000 ppm, [O_2]= 0 or 2500 ppm (total flow rate=100 cm^3 STP/min, He as balance).

100% in the whole temperature range at both 5000 and 10000 ppm of O_2, thus confirming the positive role of O_2 on this factor. By contrast, the CH_4 conversion was almost negligibly affected by the change of the O_2 content, either in the lower temperature region, where only the CH_4 combustion occurred as confirmed by the simultaneous starting of CH_4 and O_2 consumption, or at higher temperature, where the NO reduction also occurred (see Supplementary Fig.1b).

The inhibiting effect of O_2 on the NO conversion in the SCR_{NO} can be explained by taking into account two different activation processes for CH_4 and NO on the catalyst surface. If, on the one hand, the CH_4 activation is occurring on the surface of noble metal oxide-like particles [54–56], on the other hand, the NO activation occurred on a CH_4-reduced noble metal surface, this being supported by the fact that the NO reduction is starting only when O_2 was totally consumed and the surface was thus reduced by CH_4 (see Supplementary Fig. 1). This is in agreement with literature showing that the dissociation of NO to $N_{(ads)}$ and $O_{(ads)}$ takes place on a reduced noble metal surface with subsequent desorption of N_2 and removal of $O_{(ads)}$ by the reductant (CH_4 in our case) [4]. This explains why in our case on increasing the O_2 amount, which preserves the surface in the oxidised state despite the presence of a reductant (CH_4), the NO is not any longer activated and therefore converted. In particular, Rh metal in the three-way Rh-Pd-Pt-containing catalysts was found to be effective for the NO reduction under streams simulating Three-Way Catalytic Reaction, playing a relevant role in the NO dissociation [9,58]. Then, it can be suggested that Pd and Pt, which are considered to promote the CH_4 oxidation reaction [57,58] are mainly responsible for the activation of CH_4, while Rh could be responsible for NO activation.

SCR_{N2O} and CR_{N2O} reactions. The study of the N_2O abatement by CH_4 in the absence of NO and at the O_2 content of 2500 ppm, at which the best performance for SCR_{sim} was observed (SCR_{N2O}), showed that Pt,Pd,Rh/TiO_2-ZrO_2 and Pt,Pd,Rh/TiO_2-ZrO_2-CeO_2 catalysts were both active and selective for N_2O reduction (Fig. 10a and b). In particular, all the reactants (i.e. N_2O, CH_4 and O_2) started to be converted at approximately the same temperature (ca. 225°C). At 350°C, the conversions of N_2O and O_2 were complete while, at the same temperature, the CH_4 conversion reached ca. 60% with 100% CO_2 selectivity. It can be noticed that, if compared with the homologous SCR_{NO} reaction starting only when O_2 was completely consumed by CH_4, in the SCR_{N2O} the catalyst was selective for N_2O conversion with respect to combustion above 325°C up to 400°C (matching the $2N_2O + CH_4 + O_2 \rightarrow 2N_2 + CO_2 + 2H_2O$ stoichiometry), whereas below 325°C the competitive CH_4 combustion occurred to a small extent (as suggested by the stoichiometric ratios in Supplementary Fig. 2a). At higher temperature CO was also formed, leading to a decrease of CO_2 selectivity, and the CH_4 conversion increased further (up to 80 and 100% for the Pt,Pd,Rh/TiO_2-ZrO_2 and Pt, Pd,Rh/TiO_2-ZrO_2-CeO_2 catalysts, respectively, Fig. 10a and b), thus suggesting that side-reactions occurred.

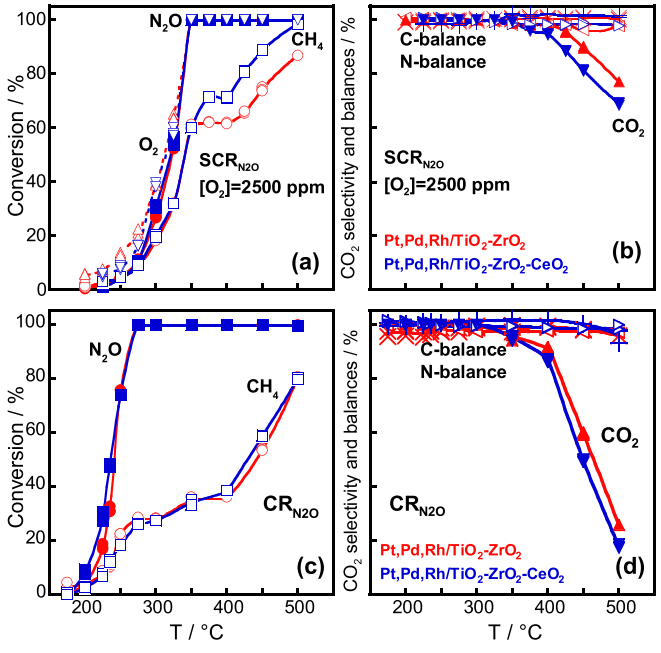

Fig. 10. SCR_{N2O} (sections a and b) and CR_{N2O} (sections c and d) reactions on Pt, Pd,Rh/TiO_2-ZrO_2 (red symbols) and Pt,Pd,Rh/TiO_2-ZrO_2-CeO_2 (blue symbols) catalysts. N_2O (●,■), CH_4 (○,□), and O_2 (△,▽) conversions as a function of temperature (Section a and c); CO_2 selectivity (▲,▼), C-balance (×,+) and N-balance (◁,▷) as a function of temperature (sections b and d). The first symbols in parentheses refer to Pt,Pd,Rh/TiO_2-ZrO_2, the second ones to Pt,Pd,Rh/TiO_2-ZrO_2-CeO_2. Reactants concentration: $[N_2O]=[CH_4]=4000$ ppm, $[O_2]=0$ or 2500 ppm (total flow rate=100 cm^3 STP/min, He as balance).

The further increase of O_2 content in the SCR_{N2O} feed from 2500 to 5000 or 10000 ppm (Supplementary Fig. 3) somewhat decreased the N_2O conversion that, at 10000 ppm, never reached completeness even at 500°C. On the other hand, O_2 in excess remarkably improved the CO_2 selectivity, which was equal to 100% in the whole temperature range explored. It is interesting to note that, at O_2 contents of 5000 and 10000 ppm, the catalyst remained very selective for N_2O reduction and the CH_4 combustion, as a side-reaction, never occurred even when O_2 was in large excess (10000 ppm), this being supported by the fact that the ratio O_2/CH_4 remained constant over the whole temperature range (Supplementary Fig. 2b and c). In particular, at 10000 ppm of O_2, O_2 is involved only in the SCR_{N2O} reaction, although with a different stoichiometry ($N_2O + CH_4 + 3/2\ O_2 \rightarrow N_2 + CO_2 + 2\ H_2O$). These results, as a whole, suggest that the N_2O always prevails on O_2 for the oxidation of active sites reduced by CH_4, i.e. O_2 does not compete with the N_2O adsorption sites.

N_2O decomposition. In order to shed more light on the N_2O-involving reactions and to get more information on the N_2O molecule activation, the N_2O decomposition was studied on both catalysts as a probe reaction. Moreover, the effect of the addition of other molecules (NO, O_2, NO + O_2) to the N_2O feed was investigated. It is well known that gaseous N_2O is dissociatively adsorbed on noble metal cationic sites having redox-properties, thus yielding N_2 and reactive surface O_{ads} species [59]. The pairing of O_{ads} species to form gaseous O_2 is generally considered as the rate-limiting step and it is strongly dependent on the O_{ads} mobility on the surface and on the strength of the O_{ads}-site bonding [59].

Both Pt,Pd,Rh/TiO_2-ZrO_2 and Pt,Pd,Rh/TiO_2-ZrO_2-CeO_2 catalysts were active for the N_2O decomposition confirming that noble-metals cationic sites characterised by a redox behaviour were present on the surface. However, a different activity can be noted as the total conversion was reached at 450°C on Pt,Pd,Rh/TiO_2-ZrO_2-CeO_2 catalyst, while in the case of Pt,Pd,Rh/TiO_2-ZrO_2 catalyst only 80% of N_2O was converted at 500°C (Fig. 11). Such a difference could be explained by the presence of CeO_2 which very likely improved the catalyst redox

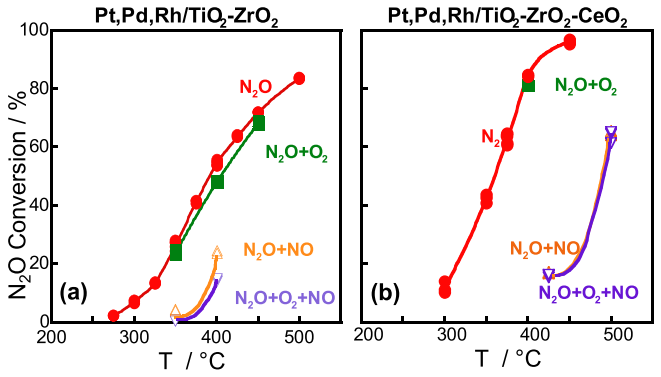

Fig. 11. N_2O abatement on Pt,Pd,Rh/TiO_2-ZrO_2 (section a) and Pt,Pd,Rh/TiO_2-ZrO_2-CeO_2 (section b). N_2O conversion *vs* temperature in N_2O decomposition or after addition to the N_2O feed of O_2 and NO, separately or together (as specified). Reactants concentration: [N_2O]=4000 ppm, [NO]=0 or 4000 ppm, [O_2]=0 or 2500 ppm (total flow rate=100 cm^3 STP/min, He as balance).

properties thus favouring the removal of O-species from the adjacent noble metal sites. This is in agreement with the known property of CeO_2 to store and release oxygen, as also evidenced in the CeO_2-ZrO_2 based catalysts [58]. In the case of the Pt,Pd,Rh/Al_2O_3-SiO_2 and Pt,Pd,Rh/Al_2O_3-ZrO_2 catalysts previously studied [27], a sigmoidal shape of N_2O conversion curve as a function of temperature was characterised by a very steep increase at about 300°C which looked like a threshold temperature. This jump was associated with a remarkable increase of the surface-O mobility, which leads to a much easier O_2 desorption, thus making free the sites for the N_2O activation. Differently from these systems [27], in the Pt,Pd,Rh/TiO_2-ZrO_2 and Pt,Pd,Rh/TiO_2-ZrO_2-CeO_2 catalysts the trend of N_2O conversion is following the Arrhenius law, thus suggesting that the surface-O mobility is not critically affected by the temperature, probably due to the effect of the different supports. By contrast, the surface-O mobility is dependent on the reactant composition.

The addition of O_2 to the N_2O feed did not change the N_2O decomposition activity, confirming our suggestion that O_2 does not compete with the N_2O adsorption sites on which the dissociative activation is proceeding (Fig. 11). It follows that, in the presence of N_2O, molecular O_2 in the gas phase does not contribute to the reactive surface-O coverage. Therefore, the O_2 inhibiting effect in the N_2O abatement by CH_4 (SCR_{N2O}, see Supplementary Fig. 3) is not related to competition between O_2 and N_2O for the same sites, but is likely due to adsorbed intermediates formed by CH_4 and O_2 (possibly carbonates) that at lower temperatures poisoned the active sites blocking surface O-species.

Differently from O_2, the addition of NO to the N_2O feed depressed the N_2O conversion, whose light-off temperature remarkably shifted from 275°C to about 350°C (Fig. 11). The addition of O_2 to the N_2O+NO mixture did not affect further the N_2O conversion. These results, as a whole, suggest that the active sites for the N_2O abatement, which are not affected by O_2, are poisoned by strongly adsorbed NO-derived species blocking surface-O species, as confirmed by the *operando*-FTIR results (vide infra).

3.5. *Operando-FTIR: surface species along N_2O and NO abatement reactions*

The evolution of the surface species formed in the presence of a flowing reactant mixture of SCR_{sim} has been studied by means of *operando*-FTIR experiments with the aim of identifying the intermediates responsible for the activity. To this purpose, the interaction of the single reactants (NO, N_2O or CH_4) and of their mixtures, with O_2 (2500 ppm) or in its absence, under reaction conditions has been investigated either at constant or at increasing temperature.

3.5.1. *NO, N_2O and CH_4 activation*

Operando-FTIR spectra collected on Pt,Pd,Rh/TiO_2-ZrO_2 as a representative sample during the N_2O decomposition at increasing temperature (Fig. 12) showed no bands of surface species besides the band of gaseous N_2O (2223 cm^{-1}), even when O_2 was added to the feed. By contrast, the addition of NO to the N_2O feed at the light-off temperature of the N_2O conversion (300°C, inset in Fig. 12) yielded either nitrosyls on noble metal sites (ν_{NO} bands at 1906 cm^{-1} of Rh-NO^+ and at 1802 cm^{-1} of Rh-NO [38–40]) and adsorbed nitrites/nitrates (bands at 1615 and 1560 cm^{-1}). Adsorbed nitrites/nitrates species were possibly in bridged configuration as their ν_3 mode, expected below 1200 cm^{-1}, was not observed in the spectra [40,60]. It should be noted that in the NO feed alone only nitrosyls and a negligible amount of nitrite/nitrate species were observed (Fig. 12). Therefore, the formation of rather large amounts of adsorbed nitrites/nitrates observed in the N_2O+NO feed can be explained suggesting that the N_2O activation occurred leaving reactive adsorbed O_{ads} species on the surface which were able to oxidize NO. These data, as a whole, can explain why the activity of the N_2O decomposition decreased when NO was added to the N_2O stream (inset in Fig. 12). Such a decrease is very likely caused by adsorbed nitrites/nitrates species which, being rather stable (bands disappeared only upon heating above 450°C), can compete with gaseous N_2O therefore blocking its adsorption/activation on some noble metal sites. The further addition of O_2 to the N_2O+NO mixture, favouring the NO oxidation to NO_2, caused the increase of amount of adsorbed nitrites/nitrates and their speciation (Fig. 12), as NO_2 can react with both reactive O-surface species of noble metal oxide-like particles and basic-O^{2-} belonging to supports. Since the activity for the N_2O abatement in the N_2O+NO feed was not affected by the O_2 addition (inset in Fig. 12), this evidence suggests that the poisoning species were only specific adsorbed nitrites/nitrates, likely those anchored on noble metal

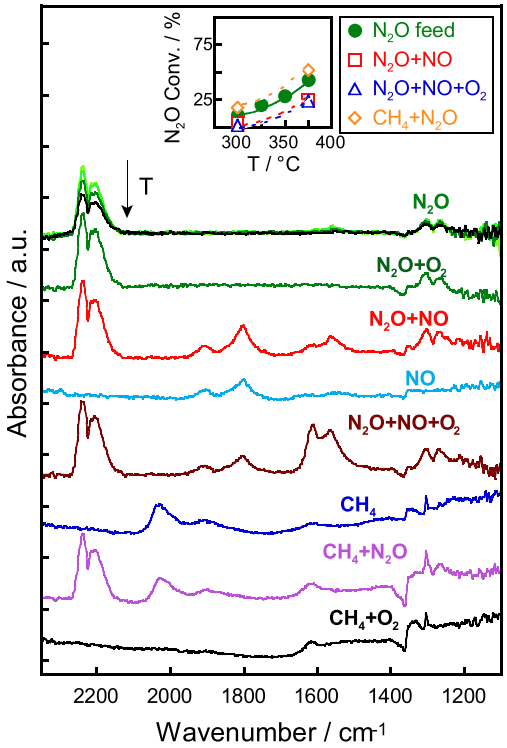

Fig. 12. *Operando*-FTIR spectra of surface species formed on activated Pt,Pd, Rh/TiO_2-ZrO_2 catalyst after saturation at 300°C under different gas mixtures (as indicated). Reactants concentration: [N_2O]=[CH_4]=[NO]=4000 ppm, [O_2]=2500 ppm (total flow=100 cm^3 STP/min, balance He). In the inset, the N_2O conversion at increasing temperature for different N_2O-containing feeds (N_2O, N_2O+NO, N_2O+NO+O_2 and CH_4+N_2O) is reported.

cationic sites.

The *operando*-FTIR experiment under CH_4 flow at 300°C (Fig. 12) showed the formation of linear and bridged carbonyls on noble metal sites (bands at 2030 and 1910 cm^{-1}, respectively). Moreover, a weak band appeared at 1615 cm^{-1} which can be possibly assigned to a formaldehyde-like species ($\nu_{(C=O)}$ in the 1750-1610 cm^{-1} region, depending on the interaction strength of the C=O with the surface, [61]), or to the incipient water (δ_{H2O}). The formation of all these bands suggests that the dissociative CH_4 activation occurred through an oxidative dehydrogenation step on reactive surface-O atoms, probably belonging to the more easily reducible PdO_x and PtO_x species with a consequent formation of their metal phases (vide supra). Upon addition of N_2O to CH_4 at 300°C, as the CR_{N2O} reaction proceeded (inset in Fig. 12), the spectrum remained almost unchanged (Fig. 12), showing the same surface species as those observed in the CH_4 feed alone with the only exception of the coupled negative/positive peaks at ca. 1370 cm^{-1} due to a side-interaction between surface species (vide supra). This suggests that the same CH_4 activation mechanism is operating also in the presence of N_2O. It follows that CH_4, acting as a reductant, can react with both the reactive surface-O released by N_2O and the surface-O belonging to the noble metal oxide which, in consequence, were reduced to the metal state, yielding the metal sites on which the H species could be adsorbed (oxidative dehydrogenation of CH_4). Finally, when O_2 is added to CH_4 at 300°C, the spectrum showed the same band from formaldehyde-like/water but the carbonyl bands disappeared, suggesting that the combustion reaction proceeded through a fast oxidation of CO surface intermediates to CO_2.

3.5.2. *Surface species during N_2O reduction with CH_4 as a function of temperature*

The study of *operando*-FTIR under the CH_4+N_2O feed at increasing temperature (Fig. 13a) showed that formaldehyde-like (or H_2O) intermediates (1615 cm^{-1}) and formate species (ν_{asym}(OCO) at 1550 cm^{-1} [62]) were already formed at 200°C, together with the coupled negative/positive peaks at ca. 1370 cm^{-1} due to side-interaction between adjacent adsorbed species (vide supra). As the temperature was increased to 250°C, the formate band disappeared while the formaldehyde band increased and bands of linear and bridged noble metal-carbonyls (2030 and 1900 cm^{-1}) appeared in the spectrum (see Fig. 13a), indicating that the complete dehydrogenation of CH_4 molecule occurred. Since at this temperature the light-off of the CH_4+N_2O reaction was observed (see inset in Fig. 13a), formates are likely playing the role of spectator species while formaldehyde and carbonyls seem to be reaction intermediates. As the temperature was increased further, the intensity of the bands belonging to carbonyls and formaldehyde (or H_2O) species went through a maximum while the catalytic activity increased (inset in Fig. 13a), in agreement with a higher reactivity of the intermediates. At temperatures higher than 400°C, a spectral baseline deformation was observed likely due to carbonaceous deposits whose amount was, however, very tiny as the C-balance was not affected (almost equal to 100%).

Operando-FTIR experiments under the CH_4+N_2O+O_2 feed (SCR_{N2O}) at increasing temperature (Fig. 13b) yielded at 200°C some absorption features ascribed to CH_xO_y species, including formaldehyde-like species (1615 cm^{-1}), two types of formate species (1580 and 1550 cm^{-1}) and methoxy species (1420 cm^{-1}). The coupled negative/positive peaks (at ca. 1360 cm^{-1}) were again observed. The absorption features related to CH_xO_y species were more complex and intense than those observed in the CH_4+N_2O feed, suggesting that the catalyst surface is kept in a higher oxidation state by O_2 leading to a higher amount of surface-O species reacting with CH_4. As in the CH_4+N_2O feed, also in the SCR_{N2O} feed, i.e. in the presence of O_2, carbonyl bands (2030 and 1910 cm^{-1}) appeared in correspondence with the reaction light-off (325°C), which, however, occurred at a temperature higher than that found for CR_{N2O} (250°C, compare insets in Fig. 13a and b). It follows that the presence of O_2 inhibited to some extent the N_2O reduction, well

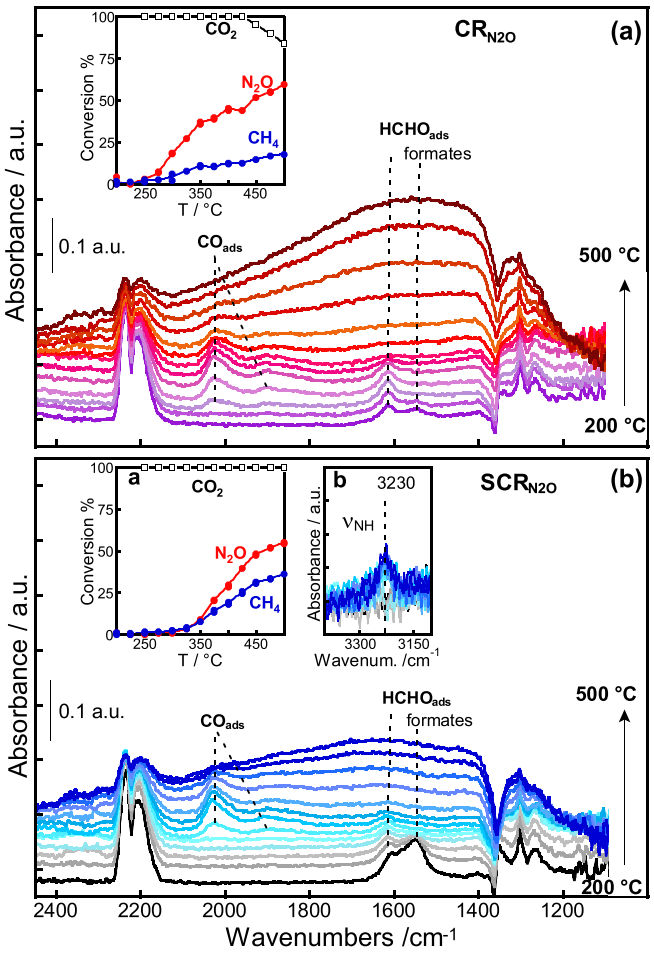

Fig. 13. *Operando*-FTIR spectra of surface species and (insets) the corresponding catalytic results (N_2O and CH_4 conversions and CO_2 selectivity *vs* T) during CR_{N2O} (section a) or SCR_{N2O} (section b) reactions at increasing temperature from 200 to 500°C (stepwise 25°C) on activated Pt,Pd,Rh/TiO_2-ZrO_2 catalyst. Reactants concentration: [N_2O]=[CH_4]=4000 ppm, [O_2]=0 or 2500 ppm (total flow rate=100 cm^3 STP/min, He as balance). In section b, the magnification of the ν_{NH} region is reported (see text).

paralleling the catalytic results obtained in the plug-flow reactor (see Supplementary Fig. 2). On increasing temperature, the spectral baseline deformation due to carbonaceous deposits is less evident than that observed in the CH_4+N_2O feed, indicating that the presence of O_2 favored, as expected, the full oxidation of such C-containing deposits, as supported by a 100% CO_2 selectivity. Interestingly, a weak band at 3230 cm^{-1}, possibly assigned to the stretching of N-H species formed on the surface [63], appears at about 300°C and its intensity remained fairly constant up to the highest temperature explored (500°C, see inset in Fig. 13b). The formation of this species results from the reaction of N-species coming from the N-N breaking of N_2O molecule with H-species coming from the CH_4 dehydrogenation, suggesting that these processes can occur along SCR of N_2O. The presence of such species supports the idea of the formation of NH_3 as a by-product which, however, formed in a very tiny amount (as the N-balance was almost 100% in the whole range of temperatures explored). It should be noted that the occurrence of the CH_4 dehydrogenation, a reaction activated by reduced species, suggests that the surface of the noble metal particles still preserved a reduced state in spite of the oxidizing condition of SCR_{N2O}.

3.5.3. *Surface species during NO reduction with CH_4 as a function of temperature*

In the NO+CH_4 feed (Fig. 14a), in the temperature range 200-275°C,

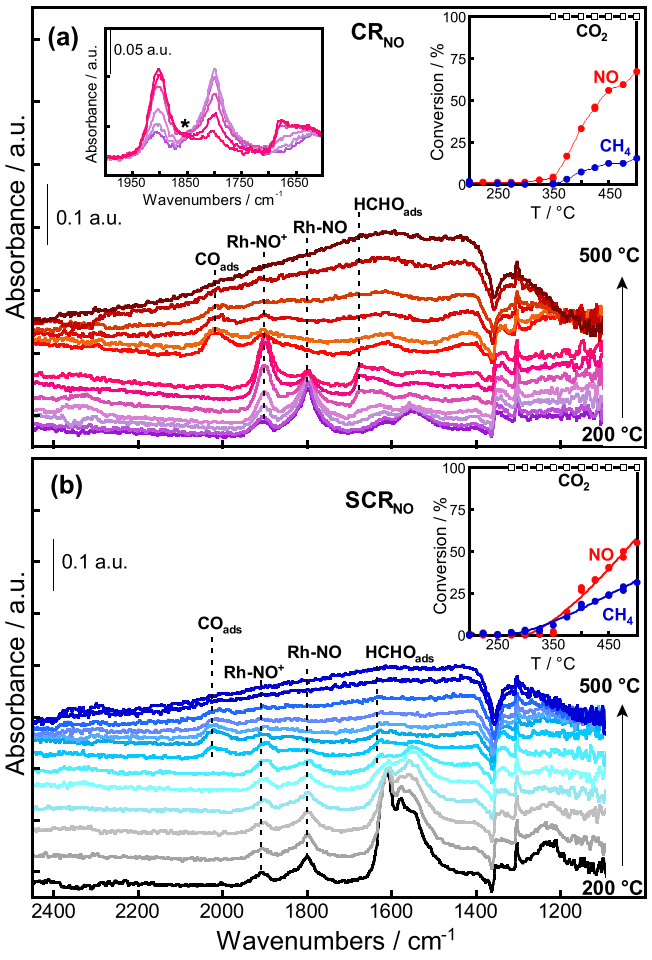

Fig. 14. *Operando*-FTIR spectra of surface species and (insets) the corresponding catalytic results (NO and CH_4 conversion and CO_2 selectivity *vs* T) during CR_{NO} (section a) or SCR_{NO} (section b) reactions at increasing temperature, from 200 to 500°C (stepwise 25°C) on activated Pt,Pd,Rh/TiO_2-ZrO_2 catalyst. Reactants concentration: [NO]=[CH_4]=4000 ppm, [O_2]=0 or 2500 ppm (total flow rate=100 cm^3 STP/min, He as balance). In section a, the magnification of the nitrosyl region showing the isosbestic point at 1850 cm^{-1} (marked with *) is reported.

well below the reaction light-off temperature of 350°C, nitrosyls bands of Rh-NO$^+$ and Rh-NO (1900 cm^{-1} and 1800 cm^{-1}, respectively) appeared in the spectra together with absorptions in the region 1615–1560 cm^{-1}, assignable to nitrite/nitrate and/or formates. On increasing temperature, but still below the light-off value, the intensity of the Rh-NO band at ca. 1800 cm^{-1} decreased while the intensity of the Rh-NO$^+$ band at ca. 1900 cm^{-1} increased. A closer analysis of the intensity of Rh-nitrosyl bands evidenced the presence of an isosbestic point at about 1850 cm^{-1} (inset in Fig. 14a), indicating that the interconversion of Rh-NO into Rh-NO$^+$ species occurred as temperature increased. This interconversion may be explained through the oxidation of Rh metal sites by the dissociative NO chemisorption, as suggested for Rh/SiO_2 and Rh/Al_2O_3 systems [38]. On increasing temperature, the intensity of the band in the region 1615–1560 cm^{-1} slightly decreased and a new band assigned to a formaldehyde-like species appeared at 1680 cm^{-1} [61], indicating that CH_4 activation is occurring thus leading to a partially oxidized surface intermediate.

Between 350°C and 375°C, surface species markedly changed due to the light-off of the CR_{NO} reaction. In particular, Rh-nitrosyls and formaldehyde (or incipient H_2O) disappeared while noble-metal linear and bridged carbonyls (bands at about 2020 and 1910 cm^{-1}) as well as a small amount of adsorbed carbonates (weak bands at about 1600 and 1400 cm^{-1}) were formed, indicating that CH_4 oxidative dehydrogenation went to completion. These findings suggest that (i) below the light-off temperature, the partial CH_4 dehydrogenation occurred together with the dissociative NO chemisorption that yielded reactive surface-O species, and (ii) at the light-off temperature, such reactive surface-O species were able to oxidize the formaldehyde-like species to carbonyls and CO_2.

In the CH_4+NO+O_2 feed at increasing temperature (SCR_{NO}, Fig. 14b), below the light-off temperature (ca. 350°C), besides Rh-nitrosyls, a large amount of nitrites/nitrates appeared in the spectra (1615–1560 cm^{-1} region) originating from the NO_2 formed in the gas phase. The nitrites/nitrates species probably hindered the formation of formaldehyde-like species and, therefore, hampered the CH_4 activation. On the other hand, as the light-off temperature was approached, the intensity of the Rh-nitrosyls and nitrites/nitrates bands decreased and the band of carbonyls (at ca. 2020 and 1910 cm^{-1}) appeared in the spectrum together with the band of the formaldehyde-like species at 1625 cm^{-1}, indicating that CH_4 activation started to occur.

3.5.4. *Surface species during NO and N_2O simultaneous reduction with CH_4 in the presence of O_2*

When N_2O and NO were co-fed with CH_4 and O_2 (SCR_{sim}), the light-off temperature for NO and N_2O conversion was the same, ca. 400°C (inset in Fig. 15). It should be noted that the light-off temperature shifted to higher temperature if compared to the values found for the separate abatement reactions (ca. 350°C for SCR_{NO} and ca. 300°C for SCR_{N2O}, see insets of Figs. 13b and 14b). This can be explained by taking into account that below the light-off temperature, besides a low amount of Rh-nitrosyls (bands at ca. 1800 and 1915 cm^{-1}), a rather large amount of nitrites/nitrates species (1615–1560 cm^{-1} region) was observed, as in SCR_{NO} (Fig. 15). Such nitrites/nitrates species could be responsible for the poisoning of active sites, by blocking the surface species reactive for CH_4, NO or N_2O activation (vide supra). This is supported by the evidence that, at the light-off temperature, the intensity of nitrites/nitrates bands remarkably decreased, likely due to their desorption, thus leaving the surface noble metal oxide species free to react. The larger shift observed for N_2O conversion light-off temperature is likely due to the competition of strongly adsorbed nitrite/nitrate species for the N_2O adsorption sites. A concomitant phenomenon likely causing the shift of the light-off to higher temperature can be the large amount of oxidants

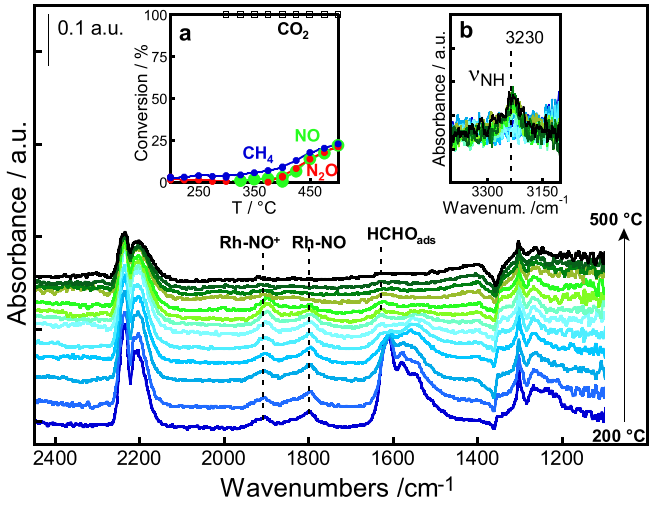

Fig. 15. *Operando*-FTIR spectra of surface species and (inset a) the corresponding catalytic results (NO, N_2O and CH_4 conversion and CO_2 selectivity) during SCR_{sim} at increasing temperature from 200 to 500°C (stepwise 25°C) on activated Pt,Pd,Rh/TiO_2-ZrO_2 catalyst. Reactants concentration: [N_2O]=[NO]=[CH_4]=4000 ppm, [O_2]=2500 ppm (total flow rate=100 cm^3 STP/min, He as balance). The magnification of the ν_{NH} region is reported in the inset b.

(N_2O, NO and O_2) which are preventing the reduction of the noble metal oxide surface species responsible in the reduced state for the CH_4 and NO activation. Moreover, approaching the light-off temperature, bands of formaldehyde-like species and formates (1630 and 1540 cm^{-1}, respectively) and, although of low intensity, of carbonyls appeared in the spectra, indicating that the CH_4 activation is starting, while the Rh-nitrosyl bands interconversion occurred, as already observed in the SCR_{NO}. Interestingly, the weak band of ν_{NH} (3230 cm^{-1} [63]) is appearing and its intensity remained fairly constant also at temperatures higher than the light-off value. Such a weak band, not found in the CR_{NO} and SCR_{NO} reactions but observed in the CR_{N2O} and SCR_{N2O} reactions above the light-off temperature, suggests a pathway in the SCR_{sim} in which the dissociative chemisorption of CH_4 and N_2O is supplying the N and H species necessary to form NH_3. This would imply the breaking of the C-H and of the N-N bonds on the noble metal sites.

As a whole, according to all the experimental findings, taking into account the high complexity of the SCR_{sim} process as well as of the catalysts on which it occurs, some considerations about the active sites and the possible pathway of NO and N_2O abatement can be suggested.

The abatement of NO and N_2O is occurring on two different active sites formed along the reaction.

The surface of noble metal oxide-like species are easily reduced by CH_4 to metals or partly reduced Me-MeO_x interfaces, as supported by the formation of CH_xO_y adsorbed species. On the surface of reduced noble metal particles, the CH_4 activation occurs through the decomposition into C and H adsorbed atoms. Such a decomposition is supported by the adsorbed very tiny amount of NH_3 formed above the light-off temperature requiring H atoms coming from the homolytic CH_4 dissociation. Moreover, the NO activation also occurs on the CH_4 reduced noble metal particles. This is enabling the NO dissociative adsorption into N and O adsorbed atoms, which can react with the CH_4-deriving C and H adsorbed species formed on adjacent noble metal sites. This last reaction step is supported by the formation of adsorbed carbonyls at the light-off of all NO-involving reactions.

The N_2O activation occurred on noble metal sites, as either surface cations or Me-MeO_x interfaces, having redox ability that is enhanced by CH_4. The reactive oxygen species coming from the N_2O decomposition step can be responsible for the CH_4 oxidative dehydrogenation to give formaldehyde-like species which will lead to CO and CO_2 possibly *via* surface carbonyls intermediates.

The presence of O_2 in the reactant stream has an inhibiting effect on the SCR_{sim} activity mainly for two reasons. First, O_2 can oxidise the reduced or partly reduced metal surface, thus inhibiting the formation of the sites active for NO and CH_4 or N_2O activation. The second reason is that O_2 reacts with gaseous NO yielding NO_2 which give rise to adsorbed nitrates intermediates poisoning the active sites at lower temperatures. On the other hand, as a positive effect, the presence of O_2 is essential for guaranteeing a complete selectivity to CO_2 thus avoiding the undesired CO formation. Therefore, for practical application it is necessary to balance adequately the amount of O_2 in the exhaust stream.

4. Conclusions

The simultaneous abatement of NO and N_2O with CH_4 in the presence of O_2 (SCR_{sim}) on both Pt,Pd,Rh/TiO_2-ZrO_2 and Pt,Pd,Rh/TiO_2-ZrO_2-CeO_2 catalysts strongly depends on the O_2/CH_4 feed ratio. Indeed, the best catalytic performance is obtained when the O_2/CH_4 ratio is less than 1 (O_2/CH_4 = 2500/4000 v/v). In such conditions, above 400°C, CH_4 efficiently and simultaneously reduces NO and N_2O with negligible formation of by-products when O_2 is almost completely consumed by combustion. As the O_2/CH_4 ratio is higher than 1 (O_2/CH_4 = 5000/4000 or 10000/4000 v/v), the SCR_{sim} becomes ineffective as the NO conversion is negligible due to CH_4 combustion which becomes the prevailing reaction. However, the presence of O_2 in the reactant stream is necessary to guarantee a good CO_2 selectivity.

Two different active sites, formed along the SCR_{sim} reaction, are suggested to be responsible for the NO and N_2O abatement with CH_4 and O_2 in the mixture in the adequate ratio. Noble-metal sites in the reduced state activate the decomposition of CH_4 and NO, while those partly reduced activate N_2O dissociation into N_2 and surface O-species. The role of CH_4 in the pathway is crucial as it likely removes reactive O-species from the surface of noble-metal oxide-like nanoparticles. The content of O_2 is critical for the catalyst surface redox properties because it hinders CH_4 in ensuring the formation of reduced or partly reduced noble-metal species that are acting as catalytic reactive centers. The *operando* FT-IR findings support this pathway view: (i) adsorbed CH_xO_y species, observed below the light-off temperature, indicate that the reduction of noble metal oxide surface occurs by stepwise CH_4 oxidative dehydrogenation; (ii) the adsorbed NH_3, observed above the light-off temperature, supports the homolytic CH_4 and N_2O (and/or NO) dissociation on the reduced noble metals surface; (iii) the formaldehyde-like and carbonyls species, formed at the light-off temperature, suggest that they likely are reaction intermediates; (iv) strongly adsorbed nitrite/nitrate species, arising from O_2 reacting with NO, account for the poisoning of active sites, blocking reactive O-species on the noble-metal oxide surface.

As the noble metal oxide-like nanoparticles are characterized by a different reducibility (Pd≥Pt≫Rh), along SCR_{sim} process, PdO_x and PtO_x oxide-like species are suggested to be more easily reduced by CH_4 at the surface, forming surface metal sites or Pd-PdO_x and Pt-PtO_x interfaces, while Rh_xO_y-like species appear to be less reducible, as indicated by Rh-NO/Rh-NO^+ species interconversion under reaction conditions.

The reduction/oxidation process of the surface noble-metal species responsible for the reactants activation is affected by the interaction with the support. Indeed, this is confirmed by the presence of CeO_2 that, even in a small amount, is improving the catalyst redox properties, through an increase of the surface O-mobility.

Finally, an assay of the catalytic behaviour in the presence of water revealed that the active sites were also preserved under these conditions, leading to a catalytic activity even slightly better that that found in the absence of water. Such evidence makes this catalysts system promising for a possible application of simultaneous abatement of NO and N_2O with CH_4 under the real conditions.

CRediT authorship contribution statement

Maria Cristina Campa: Conceptualization, Methodology, Supervision, Investigation, Data curation, Writing – original draft, Writing – review & editing. **Giuseppe Fierro:** Conceptualization, Formal analysis, Writing – original draft, Writing – review & editing. **Aidan M. Doyle:** Resources, Investigation, Writing – original draft. **Simonetta Tuti:** Investigation, Formal analysis. **Carlotta Catracchia:** Investigation, Data curation, Formal analysis. **Daniela Pietrogiacomi:** Conceptualization, Methodology, Supervision, Investigation, Data curation, Resources, Writing – original draft, Writing – review & editing, Funding acquisition.

Declaration of Competing Interest

The authors declare that they have no known competing financial interests or personal relationships that could have appeared to influence the work reported in this paper.

Data availability

Data will be made available on request.

Acknowledgments

We gratefully acknowledge 'Sapienza' University of Rome for financial support (Research Project 2016 - Grant n. RG116154E1F7B680), Dr. Sara Passeri for contributing to *Operando-*

FTIR data collections and Dr. Simona Marta (BASF Italia S.p.A., Rome) for chemical analysis.

Supplementary materials

Supplementary material associated with this article can be found, in the online version, at doi:10.1016/j.surfin.2023.103502.

References

[1] L. Alves, L.I.V. Holz, C. Fernandes, P. Ribeirinha, D. Mendes, D.P. Fagg, A. Mendes, A comprehensive review of NOx and N_2O mitigation from industrial streams, Renew. Sustain. Energy Rev. 155 (2022), 111916.

[2] A.R. Ravishankara, J.S. Daniel, R.W. Portmann, Nitrous oxide (N_2O): the dominant ozone-depleting substance emitted in the 21st century, Science 326 (2009) 123–125.

[3] M. Piumetti, S. Bensaid, D. Fino, N. Russo, Catalysis in diesel engine NO_x after treatment: a review, Catal. Struct. React. 1 (2015) 155–173.

[4] W. Shan, H. Song, Catalysts for the selective catalytic reduction of NO_x with NH_3 at low temperature, Catal. Sci. Technol. 5 (2015) 4280–4288.

[5] C. Huang, W. Shan, Z. Lian, Y. Zhang, H. He, Recent advances in three-way catalysts of natural gas vehicles, Catal. Sci. Technol. 10 (2020) 6395–6742.

[6] P. Granger, V.I. Parvulescu, Catalytic NO_x abatement systems for mobile sources: from three-way to lean burn after-treatment technologies, Chem. Rev. 111 (2011) 3155–3207.

[7] J. Song, M. Choi, J. Lee, J.M. Kim, Improvement of fuel economy and greenhouse gases reduction in gasoline powered vehicles through the TWC-NO_x trap catalyst, Int. J. Automot. Technol. 21 (2020) 441–449.

[8] S. Rood, S. Eslava, A. Manigrasso, C. Bannister, Recent advances in gasoline three way catalyst formulation: a review, Proc. Inst. Mech. Eng. Part D J. Automob. Eng. 234 (2020) 936–949.

[9] H. Asakura, S. Hosokawa, T. Ina, K. Kato, K. Nitta, K. Uera, T. Uruga, H. Miura, T. Shishido, J. Ohyama, A. Satsuma, K. Sato, A. Yamamoto, S. Hinokuma, H. Yoshida, M. Machida, S. Yamazoe, T. Tsukuda, K. Teramura, T. Tanaka, Dynamic behavior of Rh species in Rh/Al_2O_3 model catalyst during three-way catalytic reaction: an operando x-ray absorption spectroscopy study, J. Am. Chem. Soc. 140 (2018) 176–184.

[10] M. Jabłonska, R. Palkovits, It is no laughing matter: nitrous oxide formation in diesel engines and advances in its abatement over rhodium-based catalysts, Catal. Sci. Technol. 6 (2016) 7671–7687.

[11] Brochures of EnviNOx, are available at https://d2zo35mdb530wx.cloudfront.net/_legacy/UCPthyssenkruppBAIS/assets.files/products__services/fertilizer_plants/nitrate_plants/brochure-envinox_scr.pdf.

[12] G. Mul, J. Perez-Ramírez, F. Kapteijn, J.A. Moulijn, NO-Assisted N_2O Decomposition over ex-framework FeZSM-5: mechanistic aspects, Catal. Lett. 77 (2001) 7–13.

[13] J. Perez-Ramírez, F. Kapteijn, G. Mul, J.A. Moulijn, NO-assisted N_2O decomposition over Fe-based catalysts: effects of gas-phase composition and catalyst constitution, J. Catal. 208 (2002) 211–223.

[14] Y. Wu, C. Dujardin, C. Lancelot, J.P. Dacquin, V.I. Parvulescu, M. Cabie, C. R. Henry, T. Neisius, P. Granger, Catalytic abatement of NO and N_2O from nitric acid plants: a novel approach using noble metal-modified perovskites, J. Catal. 328 (2015) 236–247.

[15] R.W. van den Brink, S. Booneveld, M.J.F.M. Verhaak, F.A. de Bruijn, Selective catalytic reduction of N_2O and NO in a single reactor in the nitric acid industry, Catal. Today 75 (2002) 227–232.

[16] G.E. Marnellos, E.A. Efthimiadis, I.A. Vasalos, Simultaneous catalytic reduction of NO_x and N_2O in an In/Al_2O_3-Ru/Al_2O_3 dual-bed reactor in the presence of SO_2 and H_2O, Ind. Eng. Chem. Res. 43 (2004) 2413–2419.

[17] F. Schuricht, W. Reschetilowski, Simultaneous selective catalytic reduction (SCR) of NO_x and N_2O over Ag/ZSM-5 – catalytic studies and mechanistic implications, Micropor. Mesopor. Mater. 164 (2012) 135–144.

[18] J. Zeng, S. Chen, Z. Fan, C. Wang, H. Chang, J. Li, Simultaneous selective catalytic reduction of NO and N_2O by NH_3 over Fe-zeolite catalysts, Ind. Eng. Chem. Res. 59 (2020) 19500–19509.

[19] S.J. Lee, I.S. Ryu, S.G. Jeon, S.H. Moon, Simultaneous catalytic reduction of N_2O and NO_x for tertiary N_2O abatement technology: a field study in a nitric acid production plant, Environ. Prog. Sustain. Energy 38 (2019) 451–456.

[20] J.H. Baek, S.M. Lee, J.H. Park, J.M. Jeong, R.H. Hwang, C.H. Ko, S.G. Jeon, T. H. Choi, K.B. Yi, Effects of steam introduction on deactivation of Fe-BEA catalyst in NH_3-SCR of N_2O and NO, J. Ind. Eng. Chem. 48 (2017) 194–201.

[21] A. Guzman-Vargas, G. Delahay, B. Coq, Catalytic decomposition of N_2O and catalytic reduction of N_2O and N_2O + NO by NH_3 in the presence of O_2 over Fe-zeolite, Appl. Catal. B 42 (2003) 369–379.

[22] M. Kogel, R. Monnig, W. Schwieger, A. Tissler, T. Tureka, Simultaneous catalytic removal of NO and N_2O using Fe–MFI, J. Catal. 182 (1999) 470–478.

[23] L. Zhao, H.X. Wang, M.X. Xu, Z.S. Liu, Q. Lu, Simultaneous removal of NO and N_2O over commercial V_2O_5-MoO_3/TiO_2 catalyst modified with bismuth-nickel oxides, Appl. Catal. A General 625 (2021), 118336.

[24] M.C. Campa, D. Pietrogiacomi, C. Scarfiello, L.R. Carbone, M. Occhiuzzi, CoO_x and FeO_x supported on ZrO_2 for the simultaneous abatement of NO_x and N_2O with C_3H_6 in the presence of O_2, Appl. Catal. B Environ. 240 (2019) 367–372.

[25] M.C. Campa, D. Pietrogiacomi, M. Occhiuzzi, The simultaneous selective catalytic reduction of N_2O and NO_x with CH_4 on Co- and Ni-exchanged mordenite, Appl. Catal. B 168–169 (2015) 293–302.

[26] D. Pietrogiacomi, M.C. Campa, L. Ardemani, M. Occhiuzzi, *Operando* FTIR study of Fe-MOR, Co-MOR, and Ni-MOR as catalysts for simultaneous abatement of NO_x and N_2O with CH_4 in the presence of O_2. an insight on reaction pathway, Catal. Today 336 (2019) 131–138.

[27] M.C. Campa, A.M. Doyle, G. Fierro, D. Pietrogiacomi, Simultaneous abatement of NO and N_2O with CH_4 over modified Al_2O_3 supported Pt,Pd,Rh, Catal. Today 384-386 (2022) 76–87.

[28] D. Bounechada, G. Groppi, P. Forzatti, K. Kallinen, T. Kinnunen, Enhanced methane conversion under periodic operation over a Pd/Rh based TWC in the exhausts from NGVs, Top. Catal. 56 (2013) 372–377.

[29] G. Fierro, M. Lo Jacono, M. Inversi, P. Porta, R. Lavecchia, F. Cioci, A study of anomalous temperature-programmed reduction profiles of Cu_2O, CuO, and CuO-ZnO catalysts, J. Catal. 148 (1994) 709–721.

[30] P. Gong, J. Xie, D. Fang, X. Liu, F. He, F. Li, Novel heterogeneous denitrification catalyst over a wide temperature range: synergy between CeO_2, ZrO_2 and TiO_2, Chem. Eng. J. 356 (2019) 598–608.

[31] G. Fagherazzi, A. Benedetti, S. Polizzi, A. Di Mario, F. Pinna, M. Signoretto, N. Pernicone, Structural investigation on the stoichiometry of β-PdH_x in Pd/SiO_2 catalysts as a function of metal dispersion, Catal. Lett. 32 (1995) 293–303.

[32] M. Jablonska, TPR study and catalytic performance of noble metals modified Al_2O_3, TiO_2, and ZrO_2 for low-temperature NH_3-SCO, Catal. Comm. 70 (2015) 66–71.

[33] Y.A. Chumachenko, E.A. Buluchevskiy, E.D. Fedorova, A.A. Nepomnyashchii, T. I. Gulyaeva, M.V. Trenikhin, R.R. Izmailov, R.M. Mironenko, Hydrodeoxygenation of sorbitol to gasoline-range hydrocarbons over Pt, Pd, Rh, Ru, Ni catalysts supported on tungstated alumina, Biomass Conv. Bioref. 11 (2021) 1233–1243.

[34] S. Pitkäaho, L. Matejova, K. Jiratova, S. Ojala, R.L. Keiski, Oxidation of perchloroethylene – activity and selectivity of Pt, Pd, Rh, and V_2O_5 catalysts supported on Al_2O_3, Al_2O_3-TiO_2 and Al_2O_2-CeO_2. Part 2, Appl. Catal. B 126 (2012) 215–224.

[35] J.H. Lee, D.Y. Jo, J.W. Choung, C.H. Kim, H.C. Ham, K.Y. Lee, Roles of noble metals (M = Ag, Au, Pd, Pt and Rh) on CeO_2 in enhancing activity toward soot oxidation: Active oxygen species and DFT calculations, J. Hazard. Mater. 403 (2021) 1–12.

[36] Y. Tomida, M. Haneda, Influence of crystal structure of Y-doped ZrO_2 as support oxide on the three-way catalytic performance of supported Rh catalyst, J. Ceram. Soc. Jpn. 129 (2021) 168–174.

[37] E. Ivanova, M. Mihaylov, F. Thibault-Starzyk, M. Daturi, K. Hadjiivanov, FTIR spectroscopy study of CO and NO adsorption and co-adsorption on Pt/TiO_2, J. Mol. Catal. A Chem. 274 (2007) 179–184.

[38] S.S.C. Chuang, C.D. Tan, Combined infrared and mass spectrometric study of reactions of adsorbed NO and CO on 0.5 wt% Rh/SiO_2 catalyst, Catal. Today 35 (1997) 369–377.

[39] D.I. Kondarides, T. Chafik, X.E. Verykios, Catalytic Reduction of NO by CO over rhodium catalysts, J. Catal. 191 (2000) 147–164.

[40] K.I. Hadjiivanov, Identification of neutral and charged N_xO_y surface species by IR spectroscopy, Catal. Rev. Sci. Eng. 42 (2000) 71–144.

[41] T.J. Beck, A. Klust, M. Batzill, U. Diebold, C. Di Valentin, A. Selloni, Surface structure of TiO_2 (011)-(2x1), Phys. Rev. Lett. 93 (2004), 036104.

[42] V. Indovina, M.C. Campa, F. Pepe, D. Pietrogiacomi, S. Tuti, The catalytic activity of FeO_x/ZrO_2 and FeO_x/sulphated-ZrO_2 for the NO abatement with C_3H_6 in the presence of excess O_2, Appl. Catal. B 60 (2005) 23–31.

[43] M. Mihaylov, K. Chakarova, K. Hadjiivanov, Formation of carbonyl and nitrosyl complexes on titania- and zirconia-supported nickel: FTIR spectroscopy study, J. Catal. 228 (2004) 273–281.

[44] D. Pietrogiacomi, S. Tuti, M.C. Campa, V. Indovina, Cobalt supported on ZrO_2: catalysts characterization and their activity for the reduction of NO with C_3H_6 in the presence of excess O_2, Appl. Catal. B 28 (2000) 43–54.

[45] K.I. Hadjiivanov, IR study of CO and H_2O coadsorption on Pt^{n+}/TiO_2 and Pt/TiO_2 samples, J. Chem. Soc. Faraday Trans. 94 (1998) 1901–1904.

[46] K. Föttinger, W. Emhofer, D. Lennon, G. Rupprechter, Adsorption and reaction of CO on (Pd-)Al_2O_3 and (Pd-)ZrO_2: vibrational spectroscopy of carbonate formation, Top. Catal. 60 (2017) 1722–1734.

[47] Z.M. El-Bahy, Adsorption of CO and NO on Ceria- and Pt-Supported TiO_2: *In Situ* FTIR Study, Modern Research in Catalysis 2 (2013) 136–147.

[48] T. Chafik, D.I. Kondarides, X.E. Verykios, Catalytic reduction of NO by CO over rhodium catalysts:1. adsorption and displacement characteristics investigated by *in situ* FTIR and transient-MS techniques, J. Catal. 190 (2000) 446–459.

[49] E. Ivanova, K. Hadjiivanov, Polycarbonyls of Rh^+ formed after interaction of CO with Rh–MFI: an FTIR spectroscopic study, Phys. Chem. Chem. Phys. 5 (2003) 655–661.

[50] G. Busca, V. Lorenzelli, Infrared spectroscopic identification of species arising from reactive adsorption of carbon oxides on metal oxide surfaces, Mater. Chem. 7 (1982) 89–126.

[51] M.C. Campa, G. Ferraris, D. Gazzoli, I. Pettiti, D. Pietrogiacomi, Rhodium supported on tetragonal or monoclinic ZrO_2 as catalyst for the partial oxidation of methane, Appl. Catal. B 142-143 (2013) 423–431.

[52] J.R. González-Velasco, J.A. Botas, J.A. González-Marcos, M.A. Gutiérrez-Ortiz, Influence of water and hydrocarbon processed in feedstream on the three-way behaviour of platinum-alumina catalysts, Appl. Catal. B 12 (1997) 61–79.

[53] H. Yoshida, R. Kakei, Y. Kuzuhara, S. Misumi, M. Machida, A comparative study on TWC reactions over Rh thin films and supported Rh nanoparticles under lean conditions, Catal. Today 332 (2019) 245–250.

[54] P. Gélin, M. Primet, Complete oxidation of methane at low temperature over noble metal based catalysts: a review, Appl. Catal. B 39 (2002) 1–37.
[55] J. Yang, M. Peng, G. Ren Dr., H. Qi, X. Zhou, J. Xu, F. Deng, Z. Chen, J. Zhang Dr., K. Liu, X. Pan, W. Liu Prof., Y. Su, W. Li Prof., B. Qiao Prof., D. Ma Prof., T. Zhang Prof., A hydrothermally stable irreducible oxide-modified $Pd/MgAl_2O_4$ catalyst for methane combustion, Angew. Chem. Int. Ed. 59 (2020) 18522–18526.
[56] Y. Lu, K.A. Michalow, S.K. Matam, A. Winkler, A.E. Maegli, S. Yoon, A. Heel, A. Weidenkaff, D. Ferri, Methane abatement under stoichiometric conditions on perovskite-supported palladium catalysts prepared by flame spray synthesis, Appl. Catal. B 144 (2014) 631–643.
[57] A.W. Petrov, D. Ferri, F. Krumeich, M. Nachtegaal, J.A. van Bokhoven, O. Kröcher, Stable complete methane oxidation over palladium based zeolite catalysts, Nat. Commun. 9 (2018) 2545.
[58] J. Kašpar, P. Fornasiero, N. Hickey, Automotive catalytic converters: current status and some perspectives, Catal. Today 77 (2003) 419–449.
[59] F. Kapteijn, J. Rodriguez-Mirasol, J.A. Moulijn, Heterogeneous catalytic decomposition of nitrous oxide, Appl. Catal. B 9 (1996) 25–64.
[60] M.C. Campa, V. Indovina, D. Pietrogiacomi, The dependence of catalytic activity for N_2O decomposition on the exchange extent of cobalt or copper in Na-MOR, H-MOR and Na-MFI, Appl. Catal. B 91 (2009) 347–354.
[61] G. Busca, A.S. Elmi, P. Forzatti, Mechanism of selective methanol oxidation over vanadium oxide-titanium oxide catalysts: a FT-IR and flow reactor study, J. Phys. Chem. 91 (1987) 5263–5269.
[62] T. Nobukawa, M. Yoshida, S. Kameoka, S. Ito, K. Tomishige, K. Kunimori, *In-Situ* observation of reaction intermediate in the selective catalytic reduction of N_2O with CH_4 over Fe ion-exchanged BEA zeolite catalyst for the elucidation of its reaction mechanism using FTIR, J. Phys. Chem. B 108 (2004) 4071–4079.
[63] A.A. Davydov, Infrared Spectroscopy Of Adsorbed Species On The Surface Of Transition Metal Oxides, John Wiley & Sons; Chichester, 1990, p. 27.